ΠΑΝΕΠΙΣΤΗΜΙΟ ΠΕΙΡΑΙΩΣ
ΤΜΗΜΑ ΝΑΥΤΙΛΙΑΚΩΝ ΣΠΟΥΔΩΝ

ΣΧΟΛΗ ΝΑΥΤΙΚΩΝ ΔΟΚΙΜΩΝ
ΤΜΗΜΑ ΝΑΥΤΙΚΩΝ ΕΠΙΣΤΗΜΩΝ

ΔΠΜΣ

Διοίκηση στη Ναυτική Επιστήμη και Τεχνολογία

Διπλωματική Εργασία

“ ΣΧΕΔΙΑΣΜΟΣ ΥΠΕΡΚΡΙΣΙΜΩΝ ΚΥΚΛΩΝ RANKINE ΜΕ CO2 ΓΙΑ ΕΚΜΕΤΑΛΛΕΥΣΗ ΑΠΟΡΡΙΠΤΟΜΕΝΗΣ ΘΕΡΜΙΚΗΣ ΕΝΕΡΓΕΙΑΣ ΑΠΟ ΚΥΡΙΑ ΜΗΧΑΝΗ ΝΤΙΖΕΛ ΠΛΟΙΟΥ ΜΕΤΑΦΟΡΑΣ ΕΜΠΟΡΕΥΜΑΤΟΚΙΒΩΤΙΩΝ - ΕΠΙΛΟΓΗ ΒΕΛΤΙΣΤΟΥ ΚΥΚΛΟΥ ΜΕΣΩ ΤΕΧΝΟ-ΟΙΚΟΝΟΜΙΚΗΣ ΒΕΛΤΙΣΤΟΠΟΙΗΣΗΣ ΜΕ ΓΕΝΕΤΙΚΟ ΑΛΓΟΡΙΘΜΟ ΚΑΙ ΕΞΕΡΓΟ-ΟΙΚΟΝΟΜΙΚΗ ΚΑΙ ΕΞΕΡΓΟ-ΠΕΡΙΒΑΛΛΟΝΤΙΚΗ ΑΝΑΛΥΣΗ ΤΟΥ ”

Αθανάσιος Γ. Βάλλης

ΜΝΣΝΔ 20010

Επιβλέπων:

Δρ. Θεόδωρος Ζάννης, Αναπληρωτής Καθηγητής

Πειραιάς

Φεβρουάριος, 2022

ΔΗΛΩΣΗ ΑΥΘΕΝΤΙΚΟΤΗΤΑΣ / ΖΗΤΗΜΑΤΑ COPYRIGHT

ΤΡΙΜΕΛΗΣ ΕΞΕΤΑΣΤΙΚΗ ΕΠΙΤΡΟΠΗ:

ΜΕΛΟΣ Α΄: Θεόδωρος Ζάννης

ΜΕΛΟΣ Β΄: Ευθύμιος Παριώτης

ΜΕΛΟΣ Γ΄: Ιωάννης Κατσάνης

Ευχαριστίες

Η παρούσα διπλωματική εργασία πραγματοποιήθηκε στον Τομέα Ναυπηγικής και Ναυτικής Μηχανολογίας της Σχολής Ναυτικών Δοκίμων στο πλαίσιο του ΔΠΜΣ ‘Διοίκηση στη Ναυτική Επιστήμη και Τεχνολογία’ κατά το ακαδημαϊκό έτος 2021 – 2022. Αρχικώς θα ήθελα να ευχαριστήσω τους γονείς μου και εν γένει την οικογένεια μου για την πολύτιμη αρωγή και συμπαράσταση τους. Θα ήθελα να ευχαριστήσω ακόμη τους Καθηγητές Δρ. Θεόδωρο Ζάννη , Δρ. Ευθύμιο Παριώτη και Δρ.Ιωάννη Κατσάνη για την πολύτιμη καθοδήγηση και αρωγή τους.

Περίληψη

Στην παρούσα μελέτη διενεργείται θερμοδυναμική ανάλυση ενός Απλού υπερκρίσιμου, ενός Split υπερκρίσιμου και ενός Cascade υπερκρίσιμου κύκλου CO_2, οι οποίοι θα συνδυαστούν με τον 2χρονο κινητήρα ενός containership 6.800 TEU. Διενεργείται επίσης ανάλυση μεταφοράς θερμότητας, προκειμένου να διαστασιολογηθούν οι κατάλληλοι εναλλάκτες θερμότητας αυτών των συστημάτων. Επιπλέον, πραγματοποιείται οικονομική ανάλυση προκειμένου να υπολογιστεί το συνολικό κόστος επένδυσης αυτών των εγκαταστάσεων. Οι λειτουργικές παράμετροι αυτών των κύκλων βελτιστοποιούνται, προκειμένου να ελαχιστοποιηθεί το Κόστος Παραγωγής Ηλεκτρικής Ενέργειας (EPC), χρησιμοποιώντας γενετικό αλγόριθμο. Τα παραγόμενα αποτελέσματα από αυτές τις αναλύσεις συγκρίνονται και ο κύκλος με το χαμηλότερο EPC χρησιμοποιείται για περαιτέρω ανάλυση. Για τον επιλεγμένο κύκλο πραγματοποιείται μια παραμετρική ανάλυση προκειμένου να απεικονιστεί η διακύμανση της βελτίωσης της ειδικής κατανάλωσης καυσίμου, της παραγόμενη ισχύς και της απόδοσης του συστήματος σε διαφορετικά φορτία της μηχανής. Τέλος, για τον επιλεγμένο κύκλο διενεργείται μια εξεργοοικονομική και μια εξεργοπεριβαλλοντική ανάλυση με σκοπό τον υπολογισμό του κόστους των εξεργειακών ρευμάτων και διάφορων εξεργοπεριβαλλοντικών δεικτών.

Abstract

A thermodynamic analysis of a Simple Supercritical, a Split Supercritical and a Cascade Supercritical CO_2 cycle is conducted through the engineering software EES, which will be coupled with the 2-stroke engine of a 6.800 TEU containership. A heat transfer analysis is also conducted, in order to dimension the appropriate heat exchangers of these systems. Moreover, an economic analysis is carried out so as to calculate the total capital cost of these installations. The functional parameters of these cycles are optimized, in order to minimize the Electricity Production Cost (EPC), using genetic algorithm. The produced results from these analyses are compared and the cycle with the lowest EPC is utilized for further analysis. For the selected cycle a parametric analysis is carried out in order to illustrate the variation of the bsfc improvement, the generated power and the efficiency of the system in different engine loads. Finally, an exergoeconomic and an exergoenvironmental analysis is conducted with the intention to calculating the cost of the exergetic streams and various exergoenvironmental indicators.

Λέξεις – Κλειδιά

supercritical;EPC;genetic algorithm;optimization;exergy

Contents

Table of Figures

Tables

Nomenclature

A	Area (m^2)
A_{HX}	Heat exchanger area (m^2)
$B_{1,HX}$	Constant that is based on the heat exchanger type
$B_{2,HX}$	Constant that is based on the heat exchanger type
b	channel spacing(m)
$C_{1,HX}$	Constant that depend on the type of heat exchanger
C_{HX}^0	Bare module cost of the heat exchanger
$C_{1,C}$	Constant that is based on the compressor
$C_{2,HX}$	Constant that depend on the type of heat exchanger
$C_{2,C}$	Constant that is based on the compressor
$C_{3,HX}$	Constant that depend on the type of heat exchanger
$C_{3,C}$	Constant that is based on the compressor
C_{EXP}	Capital cost of the expander
C_{EXP}^0	Bare module cost of the expander
C_{HX}	Capital cost of the heat exchanger
C_{HX}	Capital cost of the heat exchanger
C_C	Capital cost of the compressor
C_C^0	Bare module cost of the compressor
c_p	heat capacity (J/kgK)
$\dot{C}$	cost balance rate
c	cost per exergy unit
D_h	Hydraulic port diameter (m)
f_{ei}	exergoenvironmental factor
f_k	Maintenance and insurance cost factor
$F_{M,HX}$	Material factor of heat exchanger
F_{BM}	Material factor of the compressor
F_{MP}	Additional expander factor
$F_{P,HX}$	Pressure factor of heat exchanger
$F_{P,C}$	Pressure factor of the compressor
F_S	Construction overhead cost factor
h	Convective heat transfer coefficient (W/m^2 K)
h	Specific enthalpy (J/kg)
h_{full_load}	Full load operation hours
h_{in}	Convective heat transfer coefficient of the heat exchanger internal flow (W/m^2K)
i	Interest rate
E	exergy
$K_{1,EXP}$	Constant that is based on the type of the expander

$K_{1,HX}$	Constant that is based on the heat exchanger type
$K_{1,C}$	Constant that is based on the compressor
$K_{2,EXP}$	Constant that is based on the type of the expander
$K_{2,HX}$	Constant that is based on the heat exchanger type
$K_{2,C}$	Constant that is based on the compressor
$K_{3,EXP}$	Constant that is based on the type of the expander
$K_{3,HX}$	Constant that is based on the heat exchanger type
$K_{3,C}$	Constant that is based on the compressor
k	Thermal conductivity (W/m K)
l	Length (m)
LT_{pl}	Plant lifetime
m	Mass (kg)
$\dot{m}$	Mass flow rate (kg/s)
n	Efficiency
N	Number
Nu	Nusselt number
Pr	Prandtl number
Re	Reynolds number
p	Pressure (MPa)
p_{high}	high pressure of the cycle
p_{low}	low pressure of the cycle
w_t	Power output of turbine
w_c	Power consumption of compressor
w_{net}	Net power produced
Q	Heat (J)
$\dot{Q}$	Heat transfer rate (W)
r_{in}	Fouling resistance of the heat exchanger internal flow (m^2 K/W)
r_{out}	Fouling resistance of the heat exchanger external flow (m^2 K/W)
s	Specific entropy (J/kgK)
T	Temperature (ºC)
T_0	Reference temperature of exergy destruction rate (K)
U	heat transfer coefficient (W/m^2K)
w	Channel width (m)
x	percentage of mass flow rate
Greek	
β	Rib effect coefficient or chevron angle
δ	Fin height (m)
ΔT	temperature difference (K)
ε	Convection factor or effectiveness of the heat exchanger
ε	Heat exchanger effectiveness
λ	Thermal conductivity (W/m K)
μ	Dynamic viscosity ()

θ_{ei}	environmental damage effectiveness factor

Subscripts

0	Reference
is	isentropic
recup	recuperator
heater1	heat exchanger of exhaust gas
heater2	heat exchanger of scavenge air
heater3	heat exchanger of exhaust gas
air	scavenge air
gas	exhaust gas
gas,in	exhaust gas inlet
gas,out	exhaust gas outlet
air,in	scavenge air inlet
air,out	scavenge air outlet
cond	condenser
ex	exergetic
water	sea water
water,in	sea water inlet
water,out	sea water outlet
gas,mid	exhaust gas intermediate outlet
T	turbine
C	compressor
D	destruction
cond	condenser
H	high
L	low
R	recuperator
th	thermal
in	input
ph	physical
max	maximum
min	minimum
plate	plate heat exchanger
tot	total
exergy,in	exergy input
exergy,out	exergy output
w	produced power

Dimensionless numbers

Nu	Nusselt number
Pr	Prandtl number
Re	Reynolds number

Abbreviations

bsfc	Brake specific fuel consumption
CEPCI	Chemical engineering plant cost index

CO_2	Carbon dioxide
CRF	Capital recovery factor
EPC	Electricity production cost
HT	High temperature
HX	Heat exchanger
LNG	Liquefied natural gas
LT	Low Temperature
MCT	Module cost technique
TIC	Total investment cost
TEU	twenty-foot equivalent unit
MCR	maximum continuous rating
LMTD	Logarithmic mean temperature difference

Introduction

Maritime transport is the leader of international trade due to the fact that around 80% (by volume) of global trade takes place at sea[27]. International shipping is also responsible for around 796 million tones of CO_2 , which comprises 2,2% of total greenhouse gas emissions according to the 3rd IMO GHG Study[28]. Based on this study, the growing energy demands all over the world and the general economic development will lead to an enormous increase of the CO_2 emissions,which will range between 50% to 250% by 2050. They would then constitute 12% to 18% of the total allowable CO2 emissions. In 2011, IMO decided to adopt, at the 62nd Meeting of the Marine Environment Protection Committee (MEPC), new mandatory measures in order to make ships more energy efficient. These measures were the Energy Efficiency Design Index (EEDI) for all new ships as well as the Ship Energy Efficiency Management Plan (SEEMP) for all ships in operation. This regulation has been effective since the 1st of January 2013 for ships weighing 400GT and over[29]. In 2018 at MEPC 72, IMO set a new strategy with the intention to achieving a reduction to greenhouse gases(GHG) by 40% by 2040 and at least 50% by 2050, compared to 2008. In order to achieve these targets, IMO introduced new mandatory measures ,which were the Attained Energy Efficiency Existing Ship Index(EEXI) and the annual Carbon Intensity Indicator (CII). The EEXI is calculated for ships of 400GT and over and indicates the ship’s efficiency compared to a baseline. Every ship is obliged to meet a minimum required EEXI. The CII specifies the annual reduction factor needed to provide continuous enhancement of the ship's operational carbon intensity in comparison to a specific rating level.

As it is clearly observed, regulations for CO2 emissions reduction become more and more strict. Shipping companies search new technologies to implement in ships in order to achieve the new IMO targets. An existing and very efficient technology are the waste heat recovery systems, which harness heat from sources from the engine of the ship, such as the exhaust gases, and convert it to useful electric power. These systems can utilize different thermodynamic cycles and various organic fluids,which depend on the installation where it wil be combined. Furthermore, these systems can be comprised of many different components so as to recover heat such as regenerators,evaporators and recuperators[30]. A wide range of technologies have been suggested in the literature for the exploitation of waste heat from marine diesel engines.

Liu et al. [33] investigated the potential of CO2 thermodynamic cycles to recover waste heat. In this study, were analyzed the applications which are more suitable for Transcritical and Supercritical CO2 cycles. It was examined that, Transcritical cycles suits more to low temperature heat sources and simple systems. Supercritical Cycles are more efficient for absorbing waste heat in high temperature heat sources and in more complex systems.

Nami et al.[32] performed Exergoeconomic and Exergoenvironmental analyses combining two different thermodynamic cycles, a Supercritical CO_2 Brayton cycle and an Organic Rankine cycle, in order to recover waste heat. A parametric analysis of some decision parameters was carried out, showing how they affect the exergoeconomic performance of the installation. Moreover, these parameters were optimized with intention to minimizing the capital investment cost, the exergy destruction cost and the environmental impact cost. The results of this study depicted that, the cost of the produced power is higly decreased under optimized conditions.

Liu et al.[31] proposed the utilization of a Transcritical Rankine cycle for multiple waste heat recovery using CO_2 and hydrocarbons. The optimal turbine inlet pressure was studied ed with the intention to maximizing the efficiency of the cycle and minimizing the cost of the producted electricity. For the optimal pressure , several organic fluids were examined and it was concluded that despite the fact that CO_2 does not produce the most power in comparison to the other fluids, it absorbs more heat from the renerator and the engine coolant than the other fluids and needs a smaller turbine in order to produce electricity.

Wang et al. [34] proposed a Transcritical CO2 cycle to harness heat from a Supercritical CO2 Brayton cycle and produce power. A parametric analysis is conducted in order to be showed the influence of key variables of the cycle. The exergoeconomics of the combined system are optimized and it was examined that the combined system shows better exergoeconomic performance than the simple Supercritical Cycle. Another significant point of this study is that the increase of the reactor outlet temperature decreases the total cost rate of the system.

Pan et al. [35] proposed the dual turbine-alternator- compressor Supercritical CO_2 Brayton cycle so as to recover heat from the exhaust gas of a 9000 TEU containership main engine. The functional parameters of the installation were optimized with the intention to determining the optimal operation of the system in order to maximize the efficiency of the cycle and minimize the cost of the produced power. The study illustrated that all the key performance indicators of this system are significantly better than those of the Supercritical CO2 Brayton cycle.

Su et al. [36] investigated the application of a Supercritical CO_2 cycle combined with a Transcritical CO_2 cycle for recovering waste heat from a LNG engine. The exhaust gas transfer heat subsequently in the S-CO_2 cycle and in the T-CO_2 cycle before they exit in the atmosphere. A parametric analysis was carried out in order to define the effect of operating parameters. Moreover, the optimal operating conditions of the combined system are examined taking into consideration both thermodynamic and economic aspects in the developed software. The results depicted that this system significantly in the increase of the energy and exergy efficiency of the engine.

Xia et al.[37] proposed the utilization of a simple CO_2 Rankine cycle, where the CO_2 is condensated by ‘cold’ LNG stream and is heated by ambient air. It was investigated the effect of the variation of ambient temperature and mass flow rate. It was examined that the decrease of these two parameters decreased the most of the performance indicators. It is also performed an off-design analysis, which is compared with the designed condition.

Kim et al. [38] investigated the application of three different Supercritical cycles for harnessing waste heat from a gas turbine. These three cycles are the Simple cycle, the Split cycle where the CO_2 stream is divided into streams after the compressor and the Cascade cycle where the exhaust gas transfer heat in two cycles, the High and the Low Temperature. As the results depicted, the Split is both more energetic and exergetic efficient than the other two cycles in a wide range of operating conditions.

The novelty of this work is described in the following points:

- It is investigated the application of a Simple, a Split and a Cascade Supercritical Brayton cycle in marine application, more specificly in the engine of a containership
- It is conducted for all the cycles an Energy,Exergy and Economic Analysis and the modelling of the heat exchangers through the engineering software EES
- It is utilized the genetic algorithm through the EES in order to multi-optimize the operating parameters of the cycles and it is performed a comparison between them
- For the Split cycle, which produces electricity with the lowest cost, it is conducted an Exergoeconomic and an Exergoenvironmental analysis
- It is performed a Parametric analysis in various engine loads in three different environmental conditions for the Energetic, Exergetic, Exergoeconomic and Exergonvironmental performance indicators of the Split cycle

1. Description of the 2-Stroke Engine

In the present study, the 11G90ME-C10.5 HL 2-stroke engine of the MAN is studied. It is an engine with MCR(Maximum Continuous Rating) of 68.640 kW at 84rpm, it has 3 turbochargers and is compliant with the Tier II NOx emissions[1]. Moreover, it has specific fuel consumption of 165 gr/kWh in the MCR[1]. Engine with similar characteristics has been installed in a 6800 TEU Containership, which has been studied at Byung et al [2]. The following diagrams illustrate some of the operating characteristics of the engine under study. The bsfc varies from160,1 at 70% of MCR gr/kWh to 172 gr/kWh at 25% of MCR.The exhaust gas amount increases almost linear from 55,9 kg/sec to 151,9 kg/sec as the engine load increases. The exhaust gas temperature does not change linear but increases from 221°C to 261°C until 35% of MCR, then it decreases until 220°C in 75% of MCR and finally increases until the 100% of MCR. Similar to the exhaust gas amount, the scavenge air amount increases almost linear from 55kg/sec to 148,9 kg/sec as the engine load increases. The scavenge air temperature also increases almost linear from 76°C to 214°C with the increase of MCR.

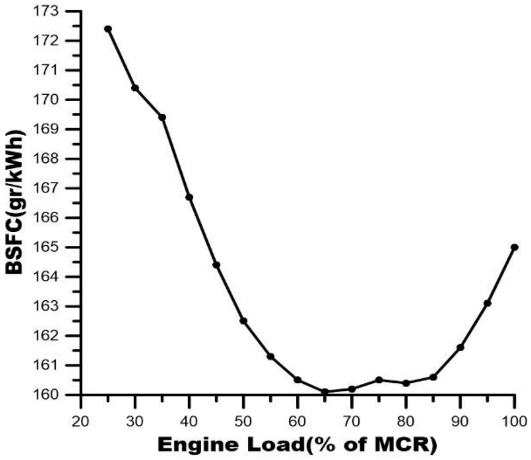

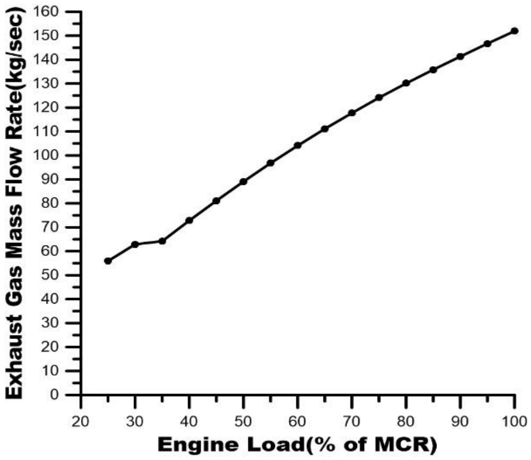

(a) (b)

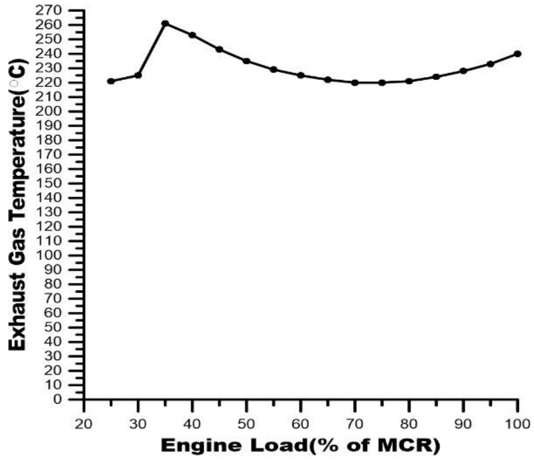

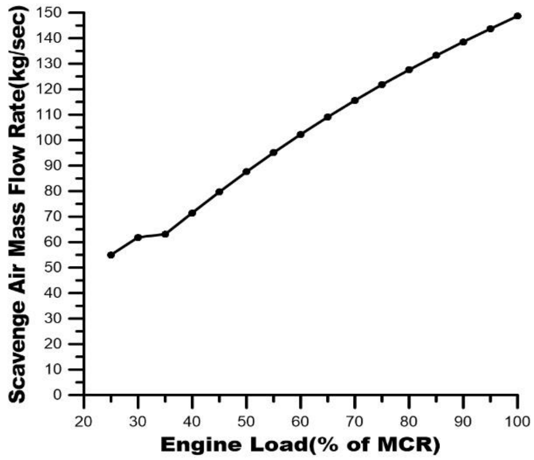

(c) (d)

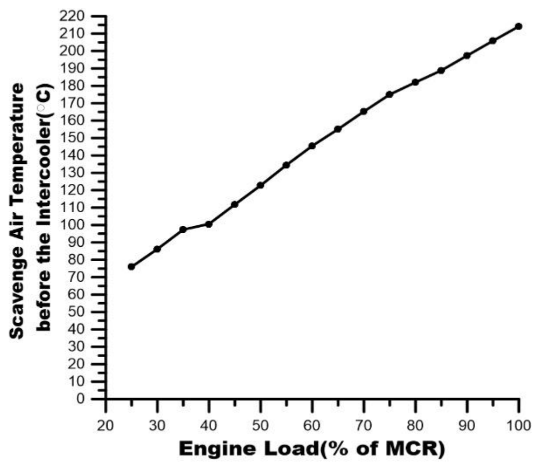

(e)

Figure 1. Variation of (a)bsfc,(b) Exhaust gas mass flow rate,(c) Exhaust gas temperature,(d) Scavenge air mass flow rate and (e) Scavenge air temperature before the intercooler with engine load. Experimental results are given for the two-stroke main marine diesel engine 11G90ME-C10.5HL

2. Briefly reference to the CO_2 Properties

The selection of the used organic fluid in a waste heat recovery system has significant meaning. The use of supercritical CO_2 cycle in waste heat recovery systems is gaining increasingly more attention due to several reasons. The supercritical CO_2 cycles operate in wide range of temperatures. Furthermore, the CO_2 is a nontoxic refrigerant and its environmental footprint is smaller in comparison to other organic fluids. Supercritical CO_2 cycles offer higher efficiencies and as a result exploit the heat source to a higher degree. In addition, the CO_2 cycles utilize heat exchangers with lower capacities, due to lower working fluid steam volume and as a consequence lead to system downsizing and decrease of the components’ capital cost [3].

Table 1. Critical Properties of CO_2

Properties	CO_2
Critical Temperature(K)	304,13
Critical Pressure (MPa)	7,37
Critical Density(kg/m^3)	467,6

3. Description of the Supercritical CO_2 Cycles

In this study, waste heat is harnessed from the intake air, after it exits the turbocharger, and from the exhaust gas of the engine. The heat exchanger of the intake air works in the same way as the intercooler of the engine but it does not reduce the temperature of the air in the same degree as the intercooler does due to the fact that the supercritical carbon dioxide cycles cannot recover heat in very low temperatures. As far as the recovered heat from the exhaust gas is concerned, in the split and in the cascade cycles two heat exchangers are utilized in order to low the exhaust gas temperature.

3.1 Description of the Simple Supercritical CO_2 Cycle

In Figure 2 is depicted the schematic view of the Simple Supercritical CO_2 Cycle and in Figure 3 the T-s diagram of this cycle. In this cycle, waste heat is harnessed from the exhaust gases of the diesel engine and from the compressed intake air, before it enters the engine’s intercooler. The installation consists of a compressor, where the supercritical CO_2 stream is compressed, a Recuperator, where the cold fluid stream is heated by the expanded hot fluid stream, two heaters, where the fluid receive heat from the intake air and the exhaust gases, an expander, where the heated CO_2 stream is expanded and a condenser, where it rejects heat in sea water so as to repeat the thermodynamic cycle. In order to enhance the thermal efficiency of the cycle, the inlet temperature of the turbine should be raised as much as possible. However, a higher turbine inlet temperature leads to a lower heat recovery efficiency of the rejected heat. For this reason, the working medium is preheated by the recuperator to a higher temperature [4] .The CO_2 stream at State 1 enters the Compressor, where it is compressed. Subsequently, at State 2 it enters the Recuperator and receives heat from the ‘hot’ CO_2 stream, which exits the Turbine at State 6. At State 3 the supercritical stream enters the Heater 1, where it receives heat from the compressed scavenge air of the engine. Afterwards, at State 4 it exits the Heater 1 and enters the Heater 2, where heat is transferred from the exhaust gas of the engine to the supercritical CO_2 stream. The stream at State 5 is expanded in the Tubrine generating power. At state 7 the CO_2 stream rejects heat in the Condenser so as to repeat the thermodynamic cycle.

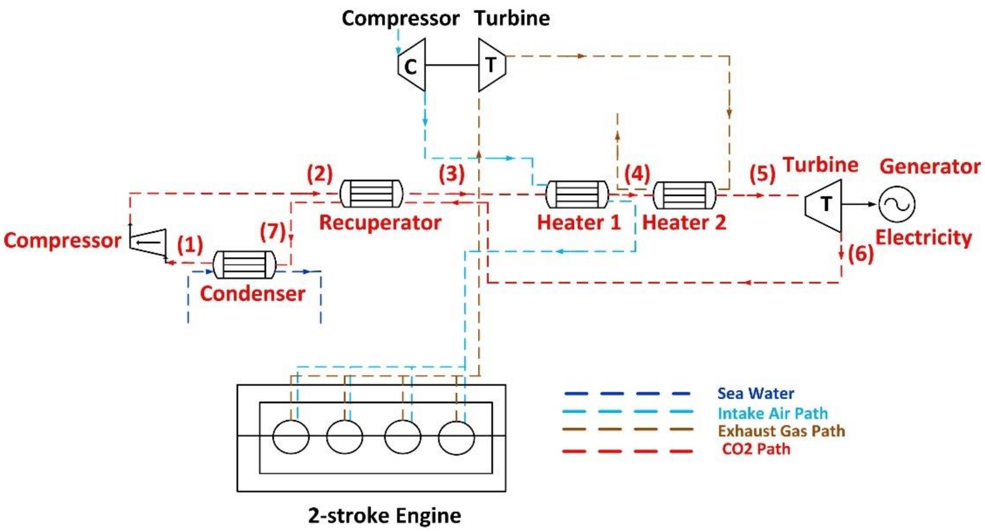

Figure 2. Schematic description of Simple Supercritical Cycle

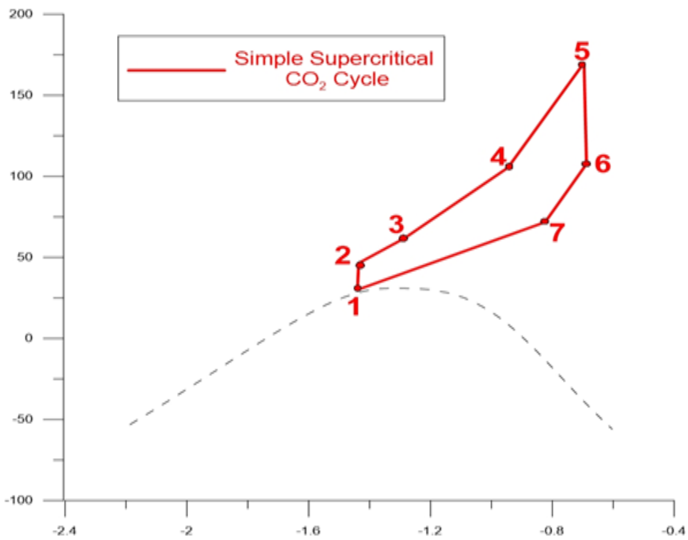

Figure 3. Diagram T-s of Simple Supercritical Cycle

3.2 Description of the Split Supercritical CO_2 Cycle

In Figure 4 is shown the schematic view of the Split Supercritical CO_2 Cycle and in Figure 5 the T-s diagram of this cycle. This installation consists of a compressor, where the supercritical CO_2 stream is compressed, a Recuperator, where a part of the ‘cold’ stream is heated by the expanded hot fluid stream,three heaters, where the stream receives heat from the intake air and the exhaust gas, an expander, where the heated CO_2 stream is expanded and a condenser, where it rejects heat in sea water. The supercritical CO_2 stream is compressed at State 1 in the Compressor. At State 2 the stream is divided into two parts.The first stream enters the Heater 1, where it recovers heat form the exhaust gases, which exit the heater in an intermediate temperature.The second stream enters the Recuperator, where it recovers heat from the ‘hot’ expanded CO_2 stream. Both streams are mixed again at State 3 and enter the Heater 2 and the Heater 3 at State 4 where they receive rejected heat from the intake air and the exhaust gases. The heated CO_2 stream at State 5 is expanded in the turbine, then at State 6 enters the recuperator and finally at State 7 is condensed in the condenser, where it rejects heat in the sea water. After the condenser, the thermodynamic cycle is repeated.

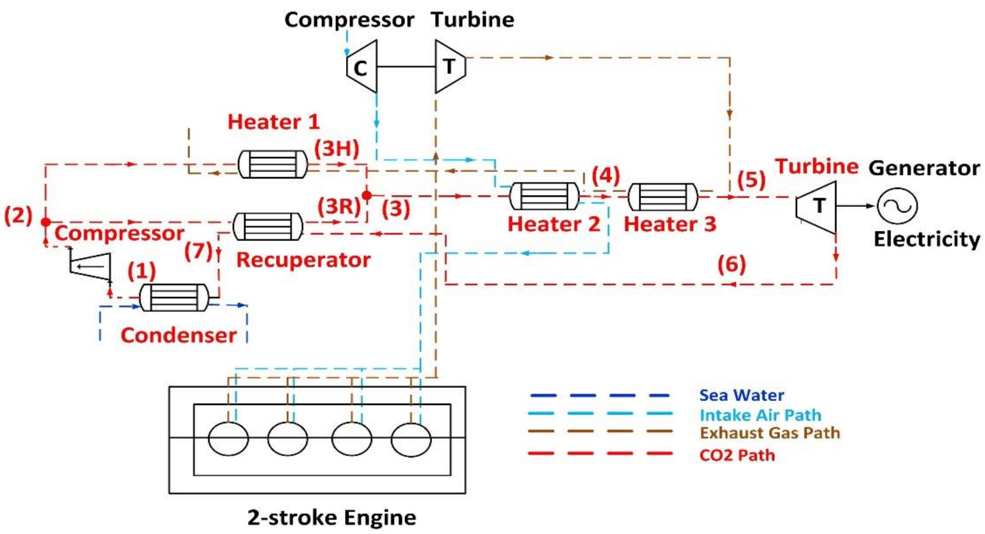

Figure 4. Schematic description of Split Supercritical Cycle

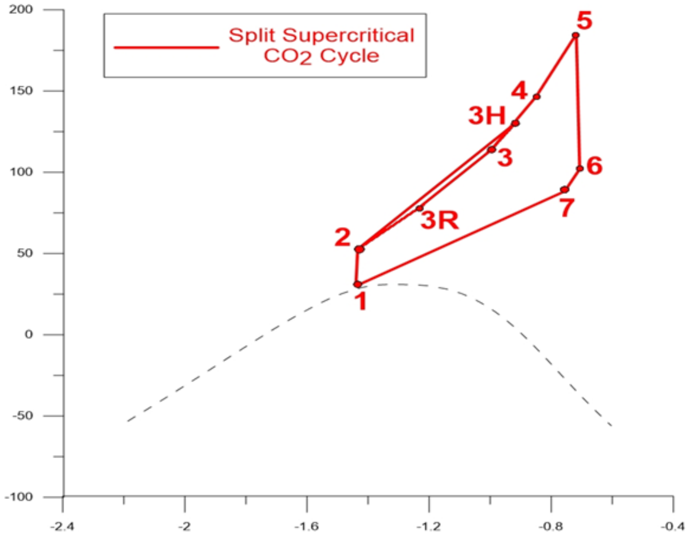

Figure 5. Diagram T-s of Split Supercritical Cycle

3.3 Description of the Cascade Supercritical CO_2 Cycle

In Figure 6 and 7 is shown the schematic view of the Cascade Supercritical CO_2 Cycle and the T-s diagram of this cycle. This installation is comprissed of a compressor, where the supercritical CO_2 stream is compressed, a Recuperator, where the HT 'cold' stream is heated by the expanded hot HT stream,three heaters, where the stream receives heat from the intake air and the exhaust gas, two expanders, where the HT and LT CO_2 streams are expanded and a condenser, where both streams reject heat in sea water. At State 1 the CO_2 stream is compressed in the compressor and at State 2 is divided into two different cycles, the High Temperature (HT) and the Low Temperature(LT). In the HT cycle, the supercritical stream recovers heat consecutively from the Recuperator, the HT Heater 1 at Sate 3H, where the rejected heat comes from the intake air before it enters the engine's intercooler and the HT Heater 2 at State 4H, where the exhaust gases reject part of their heat. The HT stream expands in the HT Turbine at State 5H, subsequently enters the Recuperator at State 6H and finally it is mixed before the Condenser with the LT stream. In the LT cycle, the stream recovers heat from the LT Heater, then at State 3L it is expanded in the LT Turbine and afterwards it is mixed with the HT stream. The mixed stream is condensated at State 8 in the condenser rejecting heat in the sea water.

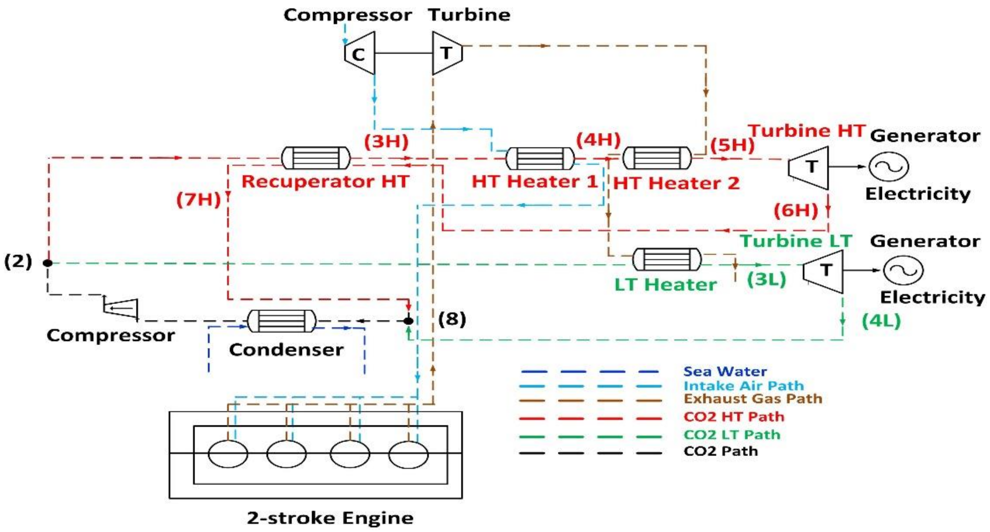

Figure 6. Schematic description of Cascade Supercritical Cycle

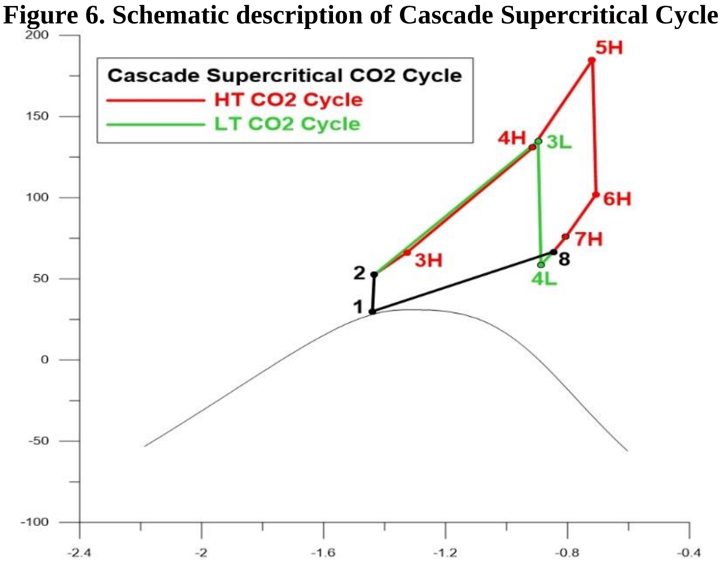

Figure 7. Diagram T-s of Cascade Supercritical Cycle

4. Energy and Exergy Analysis

4.1 Thermodynamic Processes of the Simple Supercritical Cycle

The following processes describe the Simple Supercritical Cycle, according to the Figures 3,4:

- Process 1-2: The isentropic efficiency of the compressor and the calculation of the mechanical power consumption are calculated as follows:

$$n_C = \frac{h_{2,S} - h_1}{h_2 - h_1} \tag{1}$$

$$w_C = m_{CO2}(h_2 - h_1) \tag{2}$$

- Process 2-3 and 6-7: The transferred heat in the recuperator from the ‘hot’ CO_2 stream to the ‘cold’ CO_2 stream is calculated from the following equation:

$$Q_{recup} = \varepsilon_{recup}(h_6 - h_7) = h_3 - h_2 \tag{3}$$

- Process 3-4: The transferred heat from the intake air after the turbocharger to the CO_2 stream in the Heater 1 is calculated from the following equation:

$$Q_{heater1} = \varepsilon_{heater1} m_{air} cp_{air}(T_{air,in} - T_{air,out}) = m_{CO2}(h_4 - h_3) \tag{4}$$

- Process 4-5: The transferred heat from the exhaust gas to the CO_2 stream in the Heater 2 is calculated from the following equation:

$$Q_{heater2} = \varepsilon_{heater2} m_{gas} cp_{gas}(T_{gas,in} - T_{gas,out}) = m_{CO2}(h_5 - h_4) \tag{5}$$

- Process 5-6: The isentropic efficiency of the turbine and the calculation of the produced power are depicted as follows:

$$n_T = \frac{h_5 - h_6}{h_{5,is} - h_6} \tag{6}$$

$$w_T = m_{CO2}(h_5 - h_6) \tag{7}$$

- Process 7-1: The rejected heat from the ‘hot’ CO_2 stream to the sea water in the condenser is calculated from the following equation:

$$Q_{cond} = \varepsilon_{cond} m_{CO2}(h_7 - h_1) = m_{water} cp_{water}(T_{water,out} - T_{water,in}) \tag{8}$$

4.2 Thermodynamic Processes of the Split Supercritical Cycle

The following processes describe the Split Supercritical Cycle, according to the Figures 5,6.

- Process 1-2: The isentropic efficiency of the compressor and the mechanical power consumption are calculated in the same way as in the Simple cycle.
- State 2: At this state the stream is divided in two streams, the $m_{CO2R} = x \cdot m_{CO2}$ and the $m_{CO2H} = (1-x) \cdot m_{CO2}$.
- Process 2-3R and 6-7: The transferred heat in the recuperator from the ‘hot’ CO_2 stream to the ‘cold’ CO2 stream is calculated from the following equation:
$$Q_{recup} = \varepsilon_{recup} m_{CO2}(h_6 - h_7) = m_{CO2R}(h_{3R} - h_2) \tag{9}$$
- Process 2-3H: A part of the heat from the exhaust gas is recovered in the Heater 1 and it is calculated from the following equation:

$$Q_{heater1} = \varepsilon_{heater1} m_{gas} cp_{gas} (T_{gas,mid} - T_{gas,out}) = m_{CO2H} (h_{3H} - h_2) \quad (10)$$

- State 3: Both streams are mixed at this state as follows:

$$m_{CO2} \cdot h_3 = m_{CO2R} \cdot h_{3R} + m_{CO2H} \cdot h_{3H} \quad (11)$$

- Process 3-4: The transferred heat from the intake air after the turbocharger to the CO_2 stream in the Heater 2 is calculated from the following equation:

$$Q_{heater2} = \varepsilon_{heater2} m_{air} cp_{air} (T_{air,in} - T_{air,out}) = m_{CO2} (h_4 - h_3) \quad (12)$$

- Process 4-5: The remaining heat from the exhaust gas is recovered in the Heater 3 and it is calculated as follows:

$$Q_{heater3} = \varepsilon_{heater3} m_{gas} cp_{gas} (T_{gas,in} - T_{gas,mid}) = m_{CO2} (h_5 - h_4) \quad (13)$$

- Process 5-6: The isentropic efficiency of the turbine and the calculation of the produced power are calculated in the same way as in the Simple cycle.
- Process 7-1: The rejected heat from the ‘hot’ CO_2 stream to the sea water in the condenser is calculated in the same way as in the Simple cycle.

4.3 Thermodynamic Processes of the Cascade Supercritical Cycle

The following processes describe the Cascade Supercritical Cycle, according to the Figures 7,8.

- Process 1-2: The isentropic efficiency of the compressor and the calculation of the mechanical power consumption are calculated in the same way as in the Split and the Cascade cycle.
- State 2: At this state the main cycle is divided into two cycles, the High Temperature (HT) with mass flow $m_{CO2H} = x \cdot m_{CO2}$ and the Low Temperature (LT) with mass flow $m_{CO2L} = (1-x) \cdot m_{CO2}$.
- High Temperature Stream:
    - Process 2-3H and 6H-7H: The transferred heat in the recuperator from the ‘hot’ HT CO_2 stream to the ‘cold’ HT CO_2 stream is calculated from the following equation:

$$Q_{recup,HT} = \varepsilon_{recup,HT} (h_{6H} - h_{7H}) = h_{3H} - h_{2H} \quad (14)$$

    - Process 3H-4H: The transferred heat from the intake air after the turbocharger to the HT CO_2 stream in the HT Heater 1 is calculated from the following equation:

$$Q_{heater1,HT} = \varepsilon_{heater1,HT} m_{air} cp_{air} (T_{air,in} - T_{air,out}) = m_{CO2H} (h_{4H} - h_{3H}) \quad (15)$$

    - Process 4H-5H: A part of the heat from the exhaust gas is recovered in the HT Heater 2 and it is calculated from the following equation:

$$Q_{heater2,HT} = \varepsilon_{heater2,HT} m_{gas} cp_{gas} (T_{gas,in} - T_{gas,mid}) = m_{CO2} (h_{5H} - h_{4H}) \quad (16)$$

    - Process 5H-6H: The isentropic efficiency of the HT turbine and the calculation of the produced power in the HT cycle are depicted as follows:

$$n_{T,HT} = \frac{h_{5H} - h_{6H}}{h_{5H,is} - h_{6H}} \quad (17)$$

$$w_{T,HT} = m_{CO2H} (h_{5H} - h_{6H}) \quad (18)$$

- Low Temperature Stream:
  - Process 2-3L: The remaining heat from the exhaust gas is recovered in the LT Heater and it is calculated as follows:
    $$Q_{heater,LT} = \varepsilon_{heater,LT} m_{gas} cp_{gas} (T_{gas,mid} - T_{gas,out}) = m_{CO2L} (h_{3L} - h_2) \quad (19)$$
  - Process 3L-4L: The isentropic efficiency of the LT turbine and the calculation of the produced power in the LT cycle are depicted as follows:
    $$n_{T,LT} = \frac{h_{3L} - h_{4L}}{h_{3L,is} - h_{4L}} \quad (20)$$
    $$w_{T,LT} = m_{CO2L} (h_{3L} - h_{4L}) \quad (21)$$
- State 8: At this state the HT stream and the LT stream are mixed as follows:
  $$m_{CO2} h_8 = m_{CO2H} h_{7H} + m_{CO2L} h_{4L} \quad (22)$$
- Process 8-1: The rejected heat from the 'hot' CO_2 stream to the sea water in the condenser is calculated with the following relation:
  $$Q_{cond} = \varepsilon_{cond} m_{CO2} (h_8 - h_1) = m_{water} cp_{water} (T_{water,out} - T_{water,in}) \quad (23)$$

The net generated power of each cycle is the difference between the power generated by the turbines and the consumed power by the compressors of each installation:
$$w_{net} = \sum w_{T,i} - \sum w_{P,i} \quad (24)$$
The thermal efficiency of each cycle is described by the relation below:
$$n_{th} = \frac{w_{net}}{\sum Q_{heater,i}} \quad (25)$$

4.4 Exergy Analysis

The total exergy of the stream at every point of the cycle consists of two components, the physical and the chemical exergy. The physical exergy can be assessed as follows:
$$E_{ph} = \dot{m}\left[(h_i - h_0) - T_0 (s_i - s_0)\right] \quad (26)$$
where T_0, s_0, h_0 refer to the temperature, entropy and enthalpy at the dead state.
In this study is assumed that the chemical exergy does not change from one state to another [5] and due to that reason, it has not been taken into consideration.
The exergy efficiency of the system is calculated by:
$$n_{ex} = \frac{\dot{W}_{net}}{\sum \dot{E}_{in}} \quad (27)$$

4.5 Model Assumptions

The main assumptions which are taken into account are the following:
- Each of the proposed installations operate under steady state conditions.
- Pressure drops in the pipelines are negligible.
- The isentropic efficiency of each compressor and turbine is assumed equal to 0,9.
- The effectiveness (ε) of each heat exchanger has been assumed equal to 0,9.

- At dead state T_0 and P_0 are set 27 °C and 1 bar.
- The lowest limit of the outlet temperature of the exhaust gas is set 150 ° C so as to be 30° C higher than the due point of the exhaust gas [26].

5. Modelling of Heat Exchangers

In the present study, plate heat exchanger is the selected type for the heat exchangers of the installations. The main benefits of these exchangers are their simple construction and their small size. The main drawback of plate heat exchangers is that the material which connects the plates limits their working temperature. Furthermore, the operating pressure is restricted due to the small distance of the plates. In order to define the dimensions of each heat exchanger, the required heat transfer area and the total heat transfer coefficient, a heat transfer analysis takes place below. The selected method for this analysis is the logarithmic mean temperature difference (LMTD). Based on this method, the heat transfer rate is calculated as follows:

$$\dot{Q} = U \times A \times \Delta T_{LMTD} \tag{28}$$

$$\Delta T_{LMTD} = \frac{\Delta T_{\max} - \Delta T_{\min}}{\ln(\frac{\Delta T_{\max}}{\Delta T_{\min}})} \tag{29}$$

The overall heat transfer coefficient can be calculated from the following equation:

$$\frac{1}{U_{plate}} = \frac{1}{h_{in}} + r_{in} + \frac{\delta}{\lambda} + r_{out} + \frac{1}{h_{out}} \tag{30}$$

The fouling resistance for the different fluid was set as follows:

- the fouling resistance of internal CO_2 stream r_{in} in all plate heat exchangers is set equal to 0.0002 as proposed by Cao[7].
- The fouling resistance of external intake air flow r_{out} is set equal to 0.0002 [7].
- The fouling resistance of the external exhaust gas flow r_{out} is set equal to 0.002 [7].
- The fouling resistance of the external seawater flow r_{out} is set equal to 0.00009 [7].

The convection heat transfer coefficient for the internal and external fluid is expressed by the following relation[7]:

$$h_i = \frac{kNu}{D_h} \tag{31}$$

The Nusselt number for the single-phase working fluid can be calculated from the Chisholm and Wanniarachchi [8],[9]:

$$Nu = 0.724\left(\frac{6\beta}{\pi}\right)^{0,646} Re^{0,583} Pr^{1/3} \tag{32}$$

Reynolds number is given from the following relation[8]:

$$Re = \frac{GD_h}{\mu} \tag{33}$$

The mass flux can be expressed as follows [8]:

$$G = \frac{m}{N \times w \times b} \tag{34}$$

The hydraulic diameter of the flow channel can be calculated as follows[8]:

$$D_h = \frac{4wb}{2(w+b)} \tag{35}$$

6. Economic Analysis

In this study the economic analysis takes place in order to calculate the direct and overhead costs for each component of each installation. The Module Costing Technique (MCT) is a method, which calculates the bare module cost of chemical plants [10]. According to the MCT, the capital cost of the heat exchanger can be calculated as follows:

$$C_{HX} = \frac{CEPCI_{2020}}{CEPCI_{2001}} F_S C^0_{HX} (B_{1,HX} + B_{2,HX} F_{M,HX} F_{P,HX}) \tag{36}$$

where the Chemical Engineering Plant Cost Index (CEPCI) is employed for adjusting the precise installations cost for various. $CEPCI_{2020}$ and $CEPCI_{2001}$ is the Chemical Engineering Plant Cost Index for years 2020 and 2001 respectively, C_{HX}^0 is the bare module cost of the heat exchanger, F_S is the construction overhead cost factor, $B_{1,HX}$ and $B_{2,HX}$ are the constants which base on the heat exchanger type and $F_{M,HX}$ and $F_{P,HX}$ are the material and pressure factors respectively. The value of $CEPCI_{2020}$ and $CEPCI_{2001}$ are 607.5[11] and 397 respectively[12].

The bare module cost of the heat exchanger is calculated as follows:

$$\log C^0_{HX} = K_{1,HX} + K_{2,HX} \log A_{HX} + K_{3,HX} (\log A_{HX})^2 \tag{37}$$

where $K_{1,HX}$, $K_{2,HX}$ and $K_{3,HX}$ are the constants that depend from heat exchanger type and A_{HX} is the heat exchanger area.

The pressure factor of the heat exchanger is [10]:

$$\log F_{P,HX} = C_{1,HX} + C_{2,HX} \log P_{HX} + C_{3,HX} (\log P_{HX})^2 \tag{38}$$

where $C_{1,HX}$, $C_{2,HX}$ and $C_{3,HX}$ are the constants that depend on the type of heat exchanger and P_{HX} is the design pressure of the heat exchanger.

Table 2. Values of constants for estimating the capital cost of heat exchanger[13].

Constant	Value
F_S	1.70
$B_{1,HX}$	0.96
$B_{2,HX}$	1.21
$F_{M,HX}$	2.40
$K_{1,HX}$	4,66
$K_{2,HX}$	-0,1557
$K_{3,HX}$	0,1547
$C_{1,HX}$	0
$C_{2,HX}$	0

$C_{2,HX}$	0

The capital cost of the utilized compressors is estimated as follows[10]:

$$C_C = \frac{CEPCI_{2020}}{CEPCI_{2001}} F_S C^0{}_C F_{BM} F_{P,C} \tag{39}$$

where $C^0{}_C$ is the bare module cost of the compressor, F_{BM} is the bare module factor.
The bare module cost of the compressor is[10]:

$$\log C_C^0 = K_{1,C} + K_{2,C} \log W_C + K_{3,C} (\log W_C)^2 \tag{40}$$

where $K_{1,C}$, $K_{2,C}$ and $K_{3,C}$ are the constants that depend from the type of the circulation compressor and W_C is the power consumption of the circulation compressor.

The pressure factor of the compressor can be calculated as follows:

$$\log F_{P,C} = C_{1,C} + C_{2,C} \log P_C + C_{3,C} \left(\log P_C\right)^2 \tag{41}$$

where $C_{1,C}$, $C_{2,C}$ and $C_{3,C}$ are the constants that depend on the type of the circulation compressor and P_C is the design pressure of the compressor.

Table 3. Values of constants for estimating the capital cost of compressor[13].

Constant	**Value**
F_S	1.70
F_{BM}	1.20
$K_{1,C}$	2.2897
$K_{2,C}$	1.3604
$K_{3,C}$	-0.1027
$C_{1,C}$	0
$C_{2,C}$	0
$C_{3,C}$	0

The capital cost of the expander can be expressed as follows:

$$C_{EXP} = \frac{CEPCI_{2020}}{CEPCI_{2001}} F_S C_{EXP}^0 F_{MP} \tag{42}$$

where C_{EXP}^0 is the bare module cost of the expander and F_{MP} is the additional expander factor.
The bare module cost of the expander is[10]:

$$\log C_{EXP}^0 = K_{1,EXP} + K_{2,EXP} \log W_{EXP} + K_{3,EXP} \left(\log W_T\right)^2 \tag{43}$$

where $K_{1,EXP}$, $K_{2,EXP}$ and $K_{3,EXP}$ are the constants that depend on the type of the expander, and W_T is the power output of the expander.

Table 4. Values of constants for estimating the capital cost of expander[13].

Constant	**Value**
F_{MP}	3.5
F_S	1.70
$K_{1,EXP}$	2.2659

$K_{2,EXP}$	1.4398
$K_{3,EXP}$	-0.1776

The total investment cost (TIC) of the system is the sum of the capital cost of each component of the installation:

$$C_{tot} = \sum C_{HX} + C_C + C_{EXP} \tag{44}$$

The Capital Recovery Factor (CRF) is [14]:

$$CRF = \frac{i(1+i)^{LT_{pl}}}{(1+i)^{LT_{pl}} - 1} \tag{45}$$

where i is the interest rate and LT_{pl} is the plant lifetime. The value of interest rate i is 12% [15] and the value of LT_{pl} is 15.
The Electricity Production Cost (EPC) is:

$$EPC = C_{tot} \frac{CRF + f_k}{(W_T - W_C) h_{full\_load}} \tag{45}$$

where f_k is the maintenance and insurance cost factor, which is equal to 0.06 [16] and h_{full_load} are the full load operation hours, which are 7200.

7. Multi-optimization of the Supercritical Cycles

7.1 The method of Genetic Algorithm

Genetic Algorithm is an optimization method, which gains increasingly more attention in multi-objective problems. This method is not a new one but it exists from the decade of 1960s and was developed from John Holland and his collaborators [17]. It is an probabilistic and not a minimalistic method, which is based on the genetic structure and the behavior of the chromosomes.

7.2 The Genetic Algorithm in the Supercritical Cycles

The method of Genetic Algorithm in the engineering software EES was utilized in order to set the prices of the functional parameters of the cycles so as to minimize the cost of the produced electricity (EPC) and make the investment of these installations more feasible. The load of the engine is set in the 80% of the MCR and the external conditions are considered ISO(Air Temperature=25°C,Water Temperature=25°C). It is necessary to be clarified that, the minimization of the EPC does not mean maximization of the produced power due to the fact that the EPC is dependent to the total investment cost, the produced power and the operating hours. The maximization of the produced power would lead to a significant increase of the total investment cost, which makes the investment less affordable. To conclude, the EPC was opted to be optimized so as to keep balance between the produced power and the installation cost. The parameters which were inserted in the genetic algorithm of every cycle are the following:

- the Pressure Ratio in the compressor(p_{high}/p_{low})

- the Pinch Point Temperature Difference (PPTD) in the heat exchanger of the intake air
- the Pinch Point Temperature Difference (PPTD) in the heat exchanger of the exhaust gas, where it exits in an intermediate temperature (only in the split and the cascade cycle)
- the Pinch Point Temperature Difference (PPTD) in the heat exchanger of the exhaust gas, where it exits in its final temperature
- the Pinch Point Temperature Difference (PPTD) in the recuperator
- the intermediate temperature of the exhaust gas (only in the split and the cascade cycle)
- the final temperature of the exhaust gas

The starting pressure and temperature of the stream were set at 75 bar and 30°C and the Pinch Point Temperature Difference(PPTD) in the condenser is set at 5°C.

7.3 Multi-optimization in the Simple Cycle

In the Simple Cycle, five parameters were inserted in the genetic algorithm with the following limits:

- Pressure Ratio (${}^{p_{high}}\!/\!{}_{p_{low}}$) :1,5-3,5
- PPTD in the heat exchanger of the intake air:10-30°C
- PPTD in the heat exchanger of the exhaust gas: 10-30°C
- PPTD in the recuperator: 10-30°C
- Outlet temperature of the exhaust gas:160-190°C

The results from the multi-optimization in the Simple Cycle are depicted in the Table 4. As it can be observed, the PPTD in the heat exchangers have received the value of their lowest limits except of the PPTD of the Heater 1. Moreover, the outlet temperature of the exhaust gas takes an intermediate value between the lowest and the upper limit, despite the fact that it could be set in its lowest rate in order to recover the maximum waste heat,. This can be explained because in order to minimize the EPC it is necessary to keep balance between the cost of the installation and the produced power. The thermal efficiency of the supercritical cycle is 11,07%, which is an average rate. As far as the cost of the components of the installation is concerned, the most expensive component is the compressor and the turbine follows, with the overall cost reaching the amount of 4 million Euros. As far as the cost of the produced electricity is concerned, it is 0,05637 €/kWh .

Table 5. Results from the optimization of the Simple Cycle with the genetic algorithm

Parameters	Simple Cycle
${}^{p_{high}}\!/\!{}_{p_{low}}$	2,184
$PPTD_{Recup}$ (°C)	11,6
$PPTD_{Heater1}$ (°C)	16
$PPTD_{Heater2}$ (°C)	10

$PPTD_{Cond}$ ($^{\circ}C$)	5
$T_{GAS,OUT}$ ($^{\circ}C$)	164,5
m_{CO_2} (kg/s)	71,02
w_{net} (kW)	1.899
Q_{Recup} (kW)	1.688
$Q_{Heater1}$ (kW)	8.850
$Q_{Heater2}$ (kW)	8.305
n_{th} (%)	11,07
C_{Recup} (€)	497.802
$C_{Heater1}$ (€)	569.981
$C_{Heater2}$ (€)	575.062
C_{Cond} (€)	1.119.000
C_{P} (€)	844.054
C_{EXP} (€)	419.924
C_{TOTAL} (€)	4.025.823
EPC(€/kWh)	0,05637

7.4 Multi-optimization in the Split Cycle

In the Split Cycle, eight parameters were inserted in the genetic algorithm with the following limits:

- Pressure Ratio (p_{high}/p_{low}) :2-4
- PPTD in the heat exchanger of the intake air:10-30°C
- PPTD in the intermediate heat exchanger of the exhaust gas: 10-30°C
- PPTD in the recuperator: 10-30°C
- PPTD in the final heat exchanger of the exhaust gas: 10-30°C
- Intermediate temperature of the exhaust gas:190-205°C
- Outlet temperature of the exhaust gas:150-180°C

Table 5 demonstrates the results from the multi-optimization in the Split Cycle. The value of PPTDs in the heat exchangers are in low level .The intermediate temperature of the exhaust gas almost reach its upper limit,consequently Heater 3 harness the most of the heat of the exhaust gas. The thermal efficiency of the supercritical cycle is 14%, which is a relative high rate. Despite the higher efficiency of the Split Cycle, the produced power in this cycle is less than in the Simple Cycle. As far as the components’ cost of the installation is concerned, the most expensive component is the compressor and the overall cost reach the amount of 3,3 million Euros. Moreover, the cost of the produced electricity is 0,0518 €/kWh.

Table 6. Results from the optimization of the Split Cycle with the genetic algorithm

Parameters	Split Cycle
p_{high}/p_{low}	2,679
$\mathrm{PPTD}_{Heater1}$ ($^\circ$C)	15,95
PPTD_{Recup} ($^\circ$C)	10
$\mathrm{PPTD}_{Heater2}$ ($^\circ$C)	10
$\mathrm{PPTD}_{Heater3}$ ($^\circ$C)	13,16
PPTD_{Cond} ($^\circ$C)	5
$T_{GAS,INTERMED}$ ($^\circ$C)	202
$T_{GAS,OUT}$ ($^\circ$C)	156,5
m_{CO_2} (kg/s)	42,88
x	0,346
w_{net} (kW)	1.687
Q_{Recup} (kW)	759,8
$\mathrm{Q}_{Heater1}$ (kW)	6.284
$\mathrm{Q}_{Heater2}$ (kW)	2.925
$\mathrm{Q}_{Heater3}$ (kW)	2.843
n_{th} (%)	14
C_{Recup} (€)	335.098
$C_{Heater1}$ (€)	391.797
$C_{Heater2}$ (€)	388.694
$C_{Heater3}$ (€)	380.298
C_{Cond} (€)	662.022
C_P (€)	714.459
C_{EXP} (€)	413.017
C_{TOTAL} (€)	3.285.385
EPC(€/kWh)	0,0518

7.5 Multi-optimization in the Cascade Cycle

In the Cascade Cycle, eight parameters were inserted in the genetic algorithm with the following limits:

- Pressure Ratio(p_{high}/p_{low}):1,5-3
- PPTD in the heat exchanger of the intake air:10-30°C
- PPTD in the intermediate heat exchanger of the exhaust gas: 10-30
- PPTD in the final heat exchanger of the exhaust gas: 10-30
- Intermediate temperature of the exhaust gas:190-210
- Outlet temperature of the exhaust gas:150-180

In the Table 6 the results from the optimization of the Cascade Cycle are illustrated. The final temperature of the exhaust gas receive the value of its lowest limit,subsequently this cycle harness the maximum heat. The pressure ratio receive an interemediate value.The net produced power is 2.007 kW, which is the highest value among the Supercritical Cycles and the thermal efficiency is 12,66%. The component with the highest cost of installation is the condenser and the overall cost is 4,843 million Euros. The cost of the produced electricity is 0,0642 €/kWh,which is higher than the other cycles due to the high cost of the installation .

Table 7. Results from the optimization of the Cascade Cycle with the genetic algorithm

Parameters	Cascade Cycle
p_{high}/p_{low}	2,486
$\mathrm{PPTD}_{Recup,HT}$ ($^{\circ}$C)	10
$\mathrm{PPTD}_{Heater1,HT}$ ($^{\circ}$C)	10
$\mathrm{PPTD}_{Heater2,HT}$ ($^{\circ}$C)	10
$\mathrm{PPTD}_{Heater,LT}$ ($^{\circ}$C)	15,04
PPTD_{Cond} ($^{\circ}$C)	5
$T_{GAS,INTERMED}$ ($^{\circ}$C)	199,9
$T_{GAS,OUT}$ ($^{\circ}$C)	150
m_{CO_2} (kg/s)	64,57
m_{CO_2H} (kg/s)	31,64
m_{CO_2L} (kg/s)	32,93
w_{net} (kW)	2.007
$\mathrm{Q}_{Recup,HT}$ (kW)	1.059
$\mathrm{Q}_{Heater1,HT}$ (kW)	5.383
$\mathrm{Q}_{Heater2,HT}$ (kW)	2.709
$\mathrm{Q}_{Heater,LT}$ (kW)	6.716
n_{th} (%)	12,66
$C_{Recup,HT}$ (€)	443.939
$C_{Heater1,HT}$ (€)	517.033
$C_{Heater2,HT}$ (€)	559.643
$C_{Heater,LT}$ (€)	530.759
C_{Cond} (€)	1.081.000
C_P (€)	950.281
$C_{EXP,HT}$ (€)	388.610
$C_{EXP,LT}$ (€)	372.182
C_{TOTAL} (€)	4.843.447
EPC(€/kWh)	0,06417

7.6 Results from the Multi-optimization of the Supercritical Cycles

The multi-optimization of the Supercritical Cycles with the genetic algorithm was carried out so as to find out which cycle has the lowest cost of the produced electricity. All cycles keep this cost in low level but the Split Cycle shows the lowest value as it can be noticed in Figure 8. Furthermore, Figure 9 depicts that the Split Cycle illustrates the highest energy efficiency and the lowest cost of installation but the least produced power. As far as the Simple Cycle is concerned, it reaches the second place in the cost of the produced electricity, in the produced power, in the energy efficiency and in the cost of the installation. The Cascade Cycle produces the most power but it has the highest electricity cost, the lower energy efficiency and the highest installation cost.

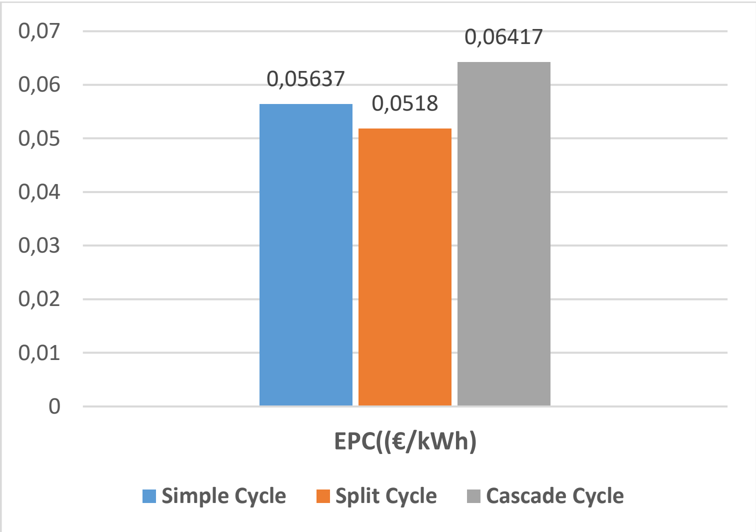

Figure 8. Electricity Production Cost(EPC) for the Supercritical Cycles

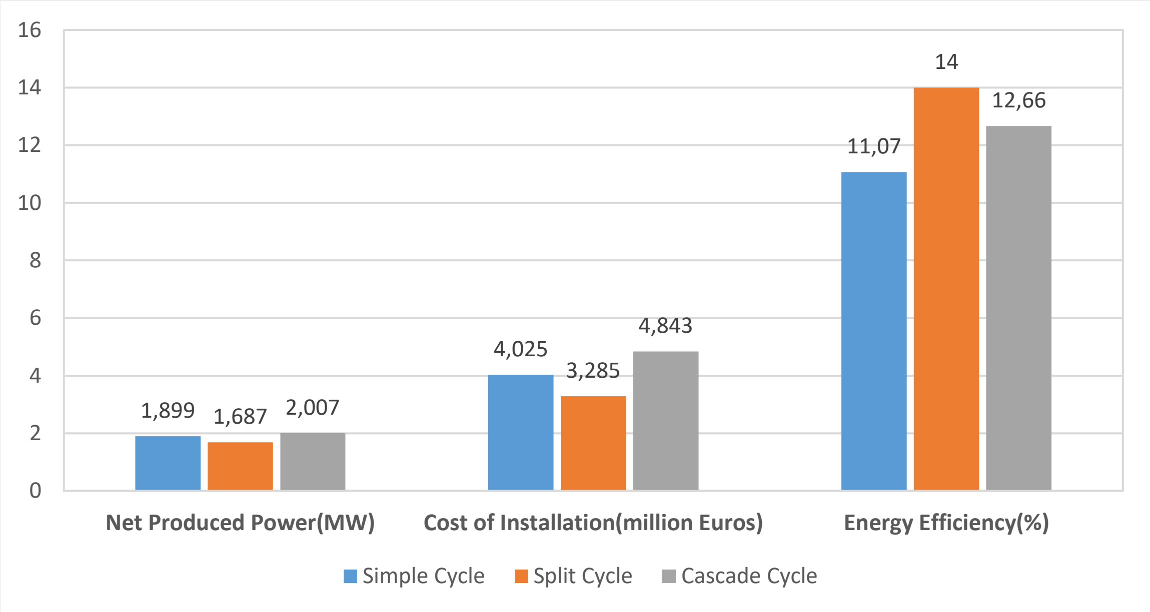

Figure 9. Net Produced Power, Cost of Installation and Energy Efficiency for the Supercritical Cycles

8. Exergoeconomic Analysis

Exergoeconomic Analysis is an analysis,which introduced by Lazzaretto and Tsatsaronis[22] that attributes cost to exergy streams in every component of the thermodynamic system based on the existing energy,exergy and economic analysis.In order to produce this analysis a cost balance equation for each component of the system has to be applied. The cost balance equation is the following[18]:

$$\sum \dot{C}_{\text{exergy,out}} + \sum \dot{C}_{w} = \sum \dot{C}_{\text{exergy,in}} + \sum \dot{Q}_{\text{th}} + \sum \dot{C}_{\text{capital,component}} \tag{46}$$

where $\dot{C}_{exergy,out}$ is the cost rate of the exergy stream that exits each component, $\dot{C}_{w}$ is the cost rate of the produced power in each component, $\dot{C}_{exergy,in}$ is the cost rate of the exergy steram that enters each component, and $\dot{C}_{capital,component}$ is the capital cost rate of each component.The previous equation can be expressed differently as follows [19]:

$$\sum (c_{\text{exergy,out}} \dot{E}_{\text{exergy,out}}) + \sum (c_{\text{w,produced}} \dot{W}_{\text{produced}}) = \sum (c_{\text{exergy,in}} \dot{E}_{\text{exergy,in}}) + \sum (c_{q,thermal} \dot{E}_{\text{q,thermal}}) + \sum \dot{C}_{\text{capital,component}} \tag{47}$$

where c_i are the costs per exergy unit. The capital cost rate $\dot{C}_{capital,component}$ of each component is calculated by the following equation [20],[21]:

$$\dot{C}_{capital,component} = \left(\frac{CRF}{h_{full\_load}} + \frac{f_k}{h_{full\_load}} \right) C_{component} \tag{48}$$

which sums the annualized investment cost and the annualized maintenance and operating cost.The value of CRF,f_k and h_{full_load} are depicted in the section of the Economic Analysis. The Table 7 illustrates a system of equations, which includes the cost balance equations and additional equations for each component. The solution of this system contains the cost rate for all the entering and exiting exergy streams and the cost per exergy unit for the producted and consumed power in each component at 80% of MCR.

$\dot{C}_{WATER,IN}, \dot{C}_{WATER,OUT}$ are set to be zero due to the fact that the cooling water is sea water, which is free in the envirronment,consequently its cost rate is negligible[21]. Furthermore $\dot{C}_{GAS,IN}, \dot{C}_{AIR,IN}$ are set to be zero[18] because of the fact that the heat is harnessed from the exhaust gas of the engine before it exits the engine and from the compressed air,before it enters the intercooler,consequently are sources of heat that are non-cost.

Table 8. Exergetic Cost Rate Balance Equations of Split Cycle[21]

Component	**Exergetic Cost Rate Balance Equation**	**Additional Equation**
Compressor	$\dot{C}_2 = \dot{C}_1 + \dot{C}_{W_C} + \dot{C}_C$	$\frac{\dot{C}_{W_C}}{W_C} = \frac{\dot{C}_{W_T}}{W_T}$
Recuperator	$\dot{C}_7 + \dot{C}_{3R} = \dot{C}_6 + \dot{C}_{2R} + \dot{C}_{recup}$	$\frac{\dot{C}_6}{E_6} = \frac{\dot{C}_7}{E_7}, \dot{C}_{2R} = x\dot{C}_2$
Heater 1	$\dot{C}_{3H} = \dot{C}_{2H} + \dot{C}_{gas,mid} + \dot{C}_{heater1}$	$\dot{C}_{2H} = (1-x)\dot{C}_2$
Heater 2	$\dot{C}_4 = \dot{C}_3 + \dot{C}_{air,in} + \dot{C}_{heater2}$	$\dot{C}_3 = \dot{C}_{3H} + \dot{C}_{3R}, \dot{C}_{air,in} = 0$
Heater 3	$\dot{C}_5 + \dot{C}_{gas,mid} = \dot{C}_4 + \dot{C}_{gas,in} + \dot{C}_{heater3}$	$\dot{C}_{gas,in} = 0, \frac{\dot{C}_5}{E_5} = \frac{\dot{C}_4}{E_4}$
Turbine	$\dot{C}_6 + \dot{C}_{W_T} = \dot{C}_5 + \dot{C}_T$	$\frac{\dot{C}_6}{\dot{E}_6} = \frac{\dot{C}_5}{\dot{E}_5}$
Condenser	$\dot{C}_1 + \dot{C}_{water,out} = \dot{C}_7 + \dot{C}_{water,in} + \dot{C}_{cond}$	$\dot{C}_{water,in} = 0, \dot{C}_{water,out} = 0$

Table 9. Cost of Exergy Streams of Split Cycle

State	Fluid	Pressure(bar)	T(°C)	Enthalpy (kJ/kg)	Entropy (kJ/kg K)	Exergy (MW)	Costs	
							$\dot{C}$(€/h)	$\dot{c}$(€/GJ)
1	CO_2	75	30	-215,1	-1,44	9,342	455,4	13,54
2	CO_2	200,93	54,64	-195,7	-1,434	10,100	517,7	14,24
3R	CO_2	200,93	74,82	-144,5	-1,282	3,587	195,1	15,12
3H	CO_2	200,93	144,1	6,079	-0,8846	7,637	322,1	11,72
3	CO_2	200,93	116	-46,13	-1,014	11,119	517,2	12,92
4	CO_2	200,93	149,6	15,39	-0,8625	11,804	527,5	12,41
5	CO_2	200,93	188,8	75,02	-0,7274	12,624	564,2	12,41
6	CO_2	75	99,51	16,25	-0,7155	9,949	444,7	12,41
7	CO_2	75	84,82	-3,465	-0,7694	9,798	437,9	12,41

The solution of the system in Table 8 utilizing the EES software leads to the results of Table 9. The objective in this Table is to depict the cost of exergy streams in each component of the system in order to find out which streams have the highest cost. As it is observed, the streams entering and exiting the Heater 3 are the most costly streams,with cost 527,4 €/h and 564,1 €/h respectively.As someone can notice, in these points the exergy of the CO_2 stream is maximized. On the other hand, the streams exiting the Recuperator and the Heater 1, are the least costly streams,they cost 179,2 €/h and 338,3 €/h respectively. In these states the exergy of the CO_2 stream is minimized. To conclude, the cost of the exergy stream seems to be proportionate to the amount of its exergy at each state.

9. Exergoenvironmental Analysis

The Exergoenvironmental Analysis is a method that contains measurements about the exergetic efficiency of the system[23-25]. In order to make this analysis, it is necessary to calculate the exergy destruction rate for each component of the Supercritical Cycle utilizing the relations of the Table 10 at 80% of MCR.

Table 10. Exergy Destruction Rate for each component of the Split Cycle[23-25]

Component	**Exergy Destruction Rate**	$\dot{E}_D$**(kW)**
Compressor	$(E_1 - E_2) + W_p$	76,4
Recuperator	$(E_{2R} - E_{3R}) + (E_6 - E_7)$	65,5
Heater 1	$(E_{2H} - E_{3H}) + (E_{gas,mid} - E_{gas,out})$	4.210
Heater 2	$(E_3 - E_4) + (E_{air,in} - E_{air,out})$	2.111
Heater 3	$(E_4 - E_5) + (E_{gas,in} - E_{gas,mid})$	1576
Turbine	$(E_5 - E_6) - W_T$	153,5
Condenser	$(E_7 - E_1) + (E_{water,in} - E_{water,out})$	456
TOTAL		8.648,4

The exergoenvironmental factor is described as the total exergy destruction rate divided into the rate of inlet exergy as follows:

$$f_{ei} = \frac{\sum \dot{E}_D}{\sum \dot{E}_{in}} \quad (49)$$

The environmental damage effectiveness factor is described as the exergoenvironmental factor divided into the exergy efficiency of the cycle as follows :

$$\vartheta_{ei} = f_{ei} \cdot C_{ei}, \quad (50)$$

where $C_{ei} = \frac{1}{n_{ex}}$ is a coefficient of exergoenvironmental impact (51)

The exergy stability factor is expressed as the total exergy destruction rate divided into the summation of total output exergy rate and total exergy destruction rate as follows:

$$f_{es} = \frac{\sum \dot{E}_D}{\sum \dot{E}x_{tot,out} + \sum \dot{E}_D + 1} \quad (52)$$

The previous parameters is preferred to reach their lowest possible value in order to exploit the maximum amount of exergy in the installation[25].

Table 11. Exergy Parameters of the Split Cycle

Exergoenvironmental Parameters	**Value**
f_{ei}	1,131
n_{ex} (%)	16,06
ϑ_{ei}	7,041
f_{es}	0,7742

10. Parametric Analysis of the Split Supercritical Cycle

The parametric analysis is carried out so as to depict the variation of various operating indicators of Split cycle as the engine load ranges from 55% to 100% of MCR in three different environmental conditions. These conditions are :

- the ISO condition, where the air temperature is 25 °C and the seawater temperature is also 25 °C
- the Specified condition, , where the air temperature is 10 °C and the seawater temperature is also 10 °C
- the Tropical condition, , where the air temperature is 45 °C and the seawater temperature is also 36 °C

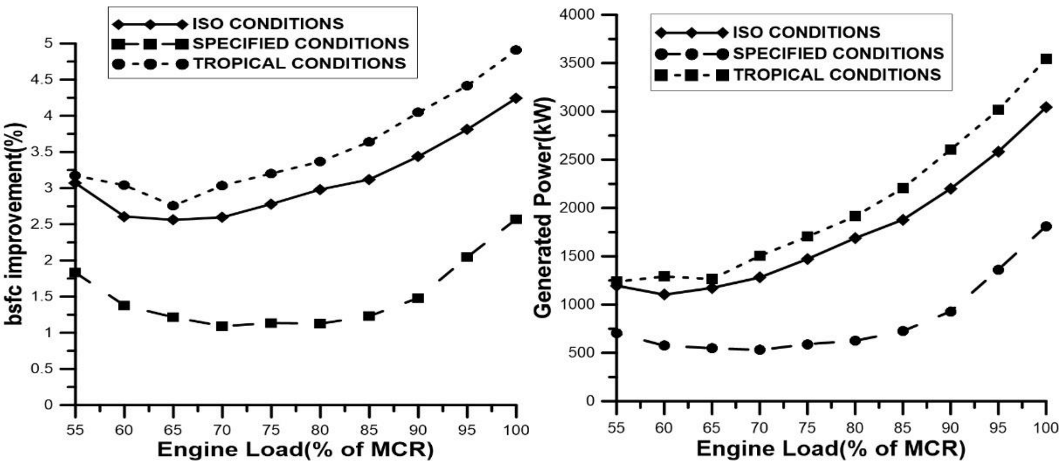

(a) (b)

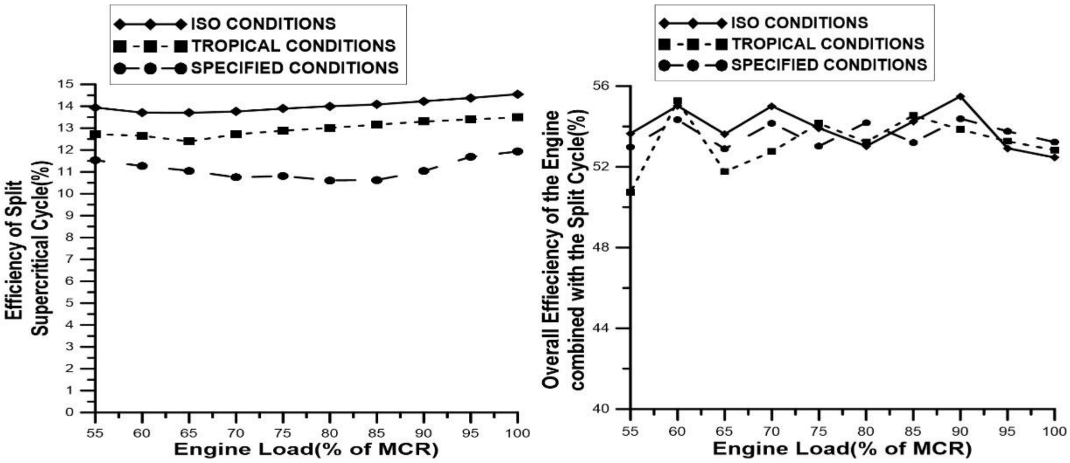

(c) (d)

Figure 10. Variation of (a) bsfc improvement, (b) generated power, (c) efficiency of the Split Supercritical Cycle, (d) overall efficiency of the engine combined with the Split Cycle with engine load in different environmental conditions

Figure 10(a) illustrates the variation of the brake specific fuel consumption(bsfc) improvement with engine load in different environmental conditions. As it is observed the bsfc is enhanced more in Tropical conditions as the engine load increases and its highest value is almost 5%. The bsfc improvement in ISO conditions follows and it reaches its highest value, which is 4,24%, as the engine load increases. The lowest bsfc improvement is noticed in Specified conditions, which the highest value is 2,6%. Figure 10(b) demonstrates the produced power in the Split cycle in different conditions. In all conditions the generated power is increased as the engine load gets higher. In Tropical conditions the most generated power is 3542 kW, in ISO conditions this value is 3040 kW and in Specified conditions this value reaches 1800 kW. Figure 10(c) illustrates the thermal efficiency of the Split cycle. As it is depicted the efficiency is slightly changed as the engine load is increased. The efficiency of this cycle ranges from 13,7% to 14,5% in ISO conditions, from 12,4% to 13,5% in Tropical conditions and from 10,6% to 11,9% in Specified conditions. Figure 10(d) shows the variation of the overall efficiency of the engine combined with the Split cycle. The overall efficiency of this installation ranges from 52,4% to 55,5% in ISO conditions, from 50,7% to 55,2% in Tropical conditions and from 52,89% to 54,4% in Specified conditions. From Figure 10 can be extracted the conclusion that in Tropical conditions the bsfc is mostly improved and it is generated the most power, whereas in ISO conditions the efficiency of the cycle is higher.

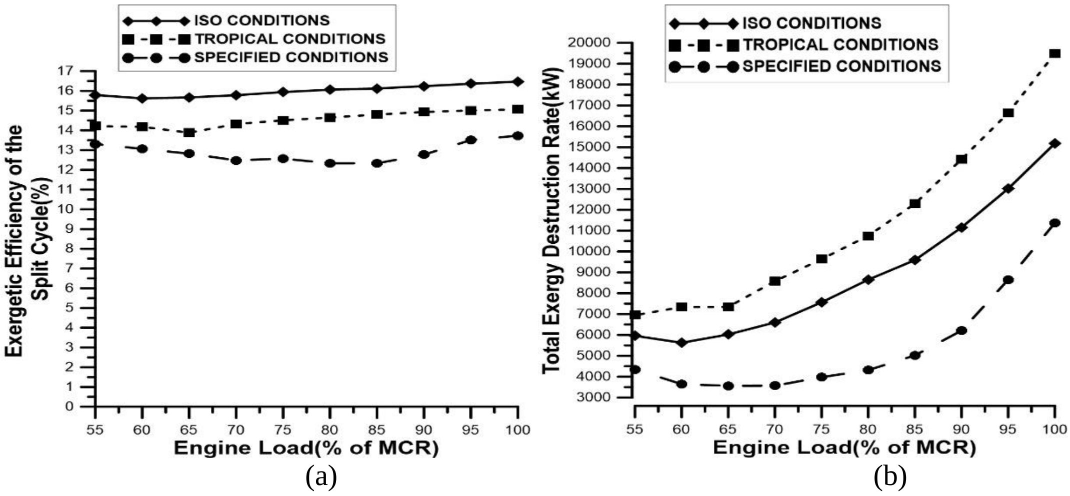

Figure 11. Variation of (a) exergy efficiency of the Split Supercritical Cycle, (b) total exergy destruction rate of the Split Supercritical Cycle in different environmental conditions

Figure 11(a) demonstrates the variation of exergetic efficiency of the Split cycle in different conditions. In ISO and Tropical conditions is almost kept stable as engine load changes. The highest exergetic efficiency is depicted in ISO conditions, where it ranges from 15,6% to 16,5%. In Tropical conditions the efficiency varies from 13,9% to 15,1% and in Specified conditions ranges from 12,3% to 13,7%. Figure 10(b) illustrates the variation of total exergy destruction rate, which is increased as the engine load is increased. The lowest destruction is depicted in Specified conditions, in which the lowest value is 3.560 kW and the highest value is 11.370 kW. In ISO conditions the total exergy destruction rate ranges from 5.630 kW to 15.200 kW. In Tropical conditions the total exergy destruction rate ranges from 6.948 kW to 19.487 kW.

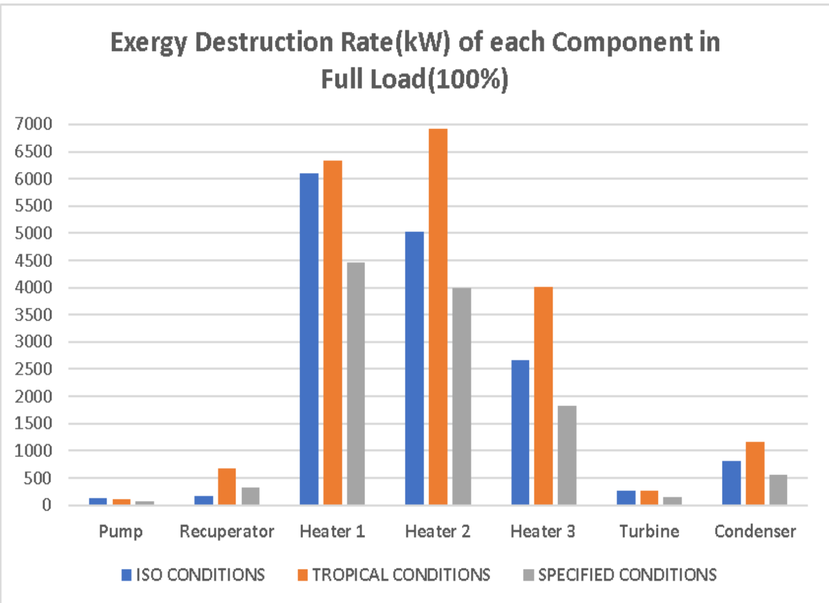

(a)

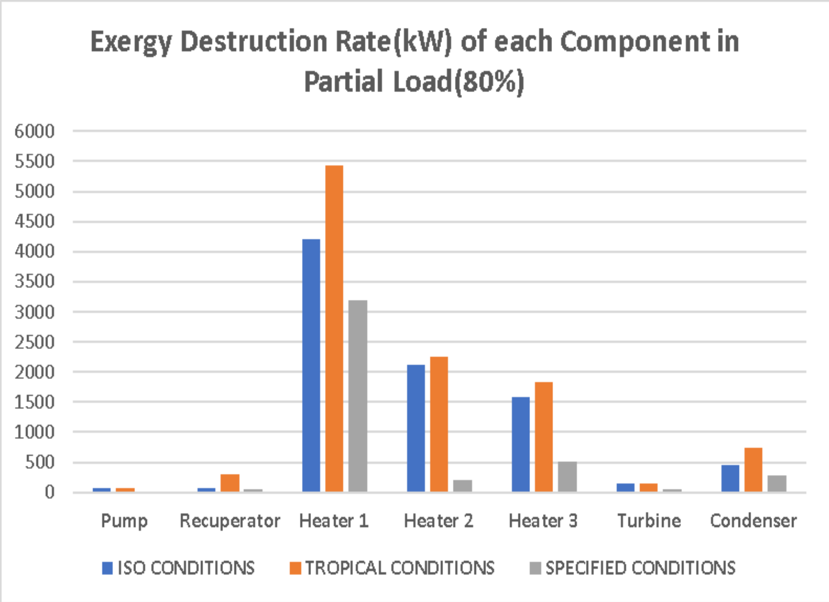

(b)

Figure 12. Variation of (a) exergy destruction rate of each component in full load , (b) exergy destruction rate of each component in partial load in different environmental conditions

Figure 12(a),(b) deomonstrates the exergy destruction rate of each component in full load and in 80% of MCR. As it can be noticed, the destruction rate in the compressor, the recuperator, the turbine and the condenser are in significant low levels and do not highly differ in full and in partial load. On the other side, Heater1,2 and 3 are mainly responsible for the total exergy destruction rate. All of the components have the maximum exergy destruction rate in tropical conditions, which is reasonable due to the Figure 11. In full load Heater 2 illustrates the highest destruction rate, which is almost 7.000 kW, Heater 1 is in 2nd place with almost 6.500 kW and Heater 3 in 3rd place with 4.000 kW. In 80% of MCR (partial load) Heater 1 depicts the highest destruction rate with almost 5.500 kW, Heater 2 is in 2nd place with 2.250 kW and Heater 3 is in 3rd place with 1.800 kW. The exergy destruction rate of Heater 1 does not highly differ due to the fact that the intermediate and the outlet temperature of exhaust gas does not change in different loads. On the contrary, the exergy destruction rate Heater 2 and 3 higly differ because of the fact that the inlet temperature of exhaust gas changes significantly.

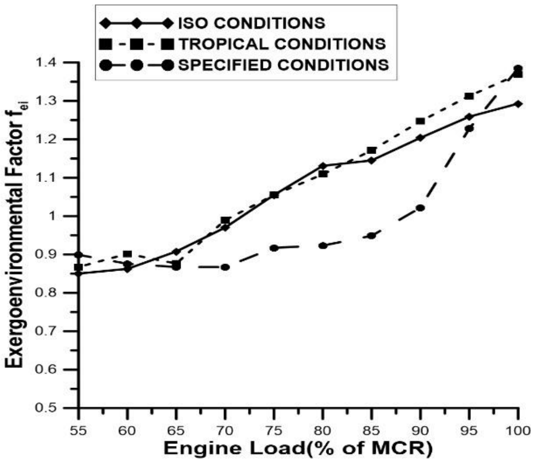

(a)

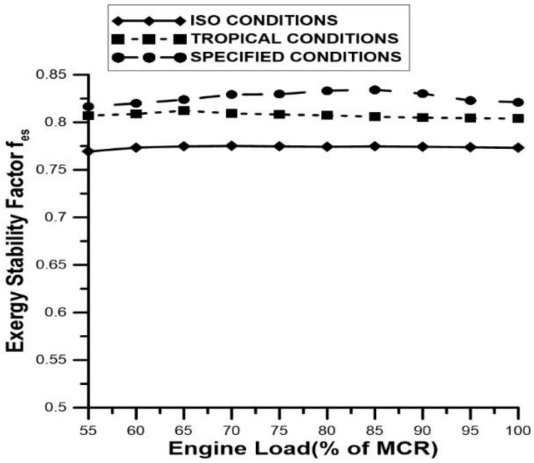

(b)

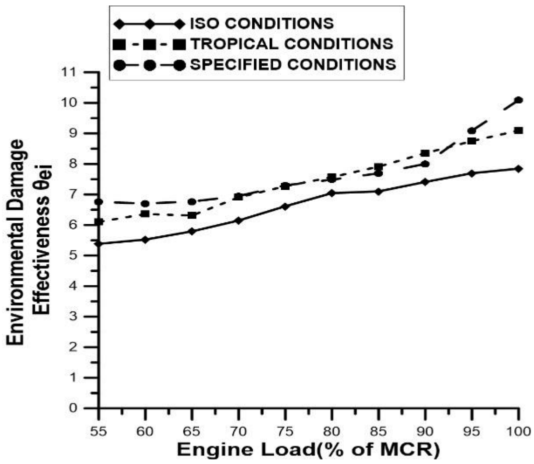

(c)

Figure 13. Variation of (a) Exergoenvironmental factor, (b) Exergy Stability factor, (c) Environmental Damage effectiveness with engine load in different environmental conditions

Figure 13(a) illustrates the variation of exergoenvironmental factor in different conditions. The exergoenvironmental factor is increased as the engine load reaches higher values. In ISO conditions the exergoenvironmental factor ranges from 0,85 to 1,29, in Tropical conditions varies from 0,87 to 1,37 and in Specified conditions varies from 0,87 to 1,39. Figure 13(b) demonstrates the variation of exergy stability factor in different conditions. These factor is almost kept stable as the engine load is increased. In ISO conditions the exergy stability factor ranges from 0,77 to 0,78 , in Tropical conditions varies from 0,80 to 0,81 and in Specified conditions varies from 0,81 to 0,83. Figure 13(c) depicts the variation of environmental damage effectiveness. In ISO conditions the environmental damage effectiveness ranges from 5,4 to 7,85 , in Tropical conditions varies from 6,1 to 9,1 and in Specified conditions varies from 6,7 to 10,1. These factors are the basis of exergoenvironmental analysis and it is desirable to reach their lowest value. As it is obvious, in ISO conditions these factors reach their lowest value.

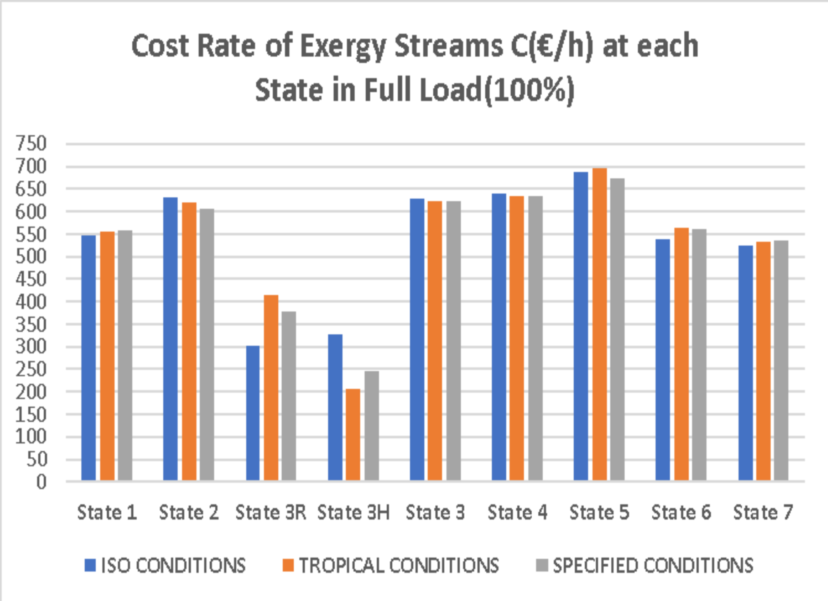

(a)

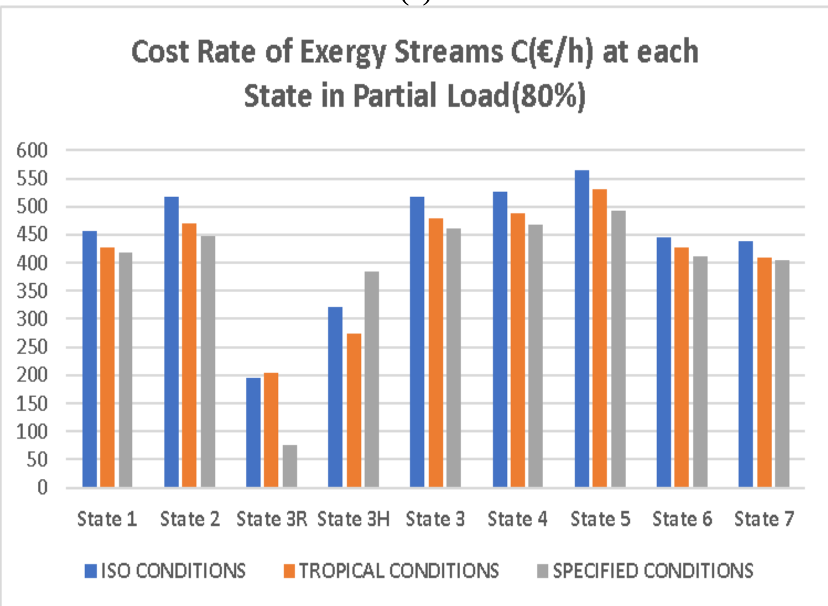

(b)

Figure 14. Variation of cost rate of exergy streams at each state (a) in full load , (b) in partial load in different environmental conditions

Figure 14 illustrates the cost rate of exergy streams at each state of Split cycle in full and in partial load in different conditions. The lowest cost rate is depicted at state 3R in partial load and at state 3H in full load. The highest cost rate is noticed at state 5 in both loads.The conditions do not change significantly the value of cost rate at most states, but in partial load and in ISO conditions the cost rate is slightly higher than the other conditions in almost every state. Furthermore, it also noticed that in full load every state has higher cost rate with exception to state 3R.

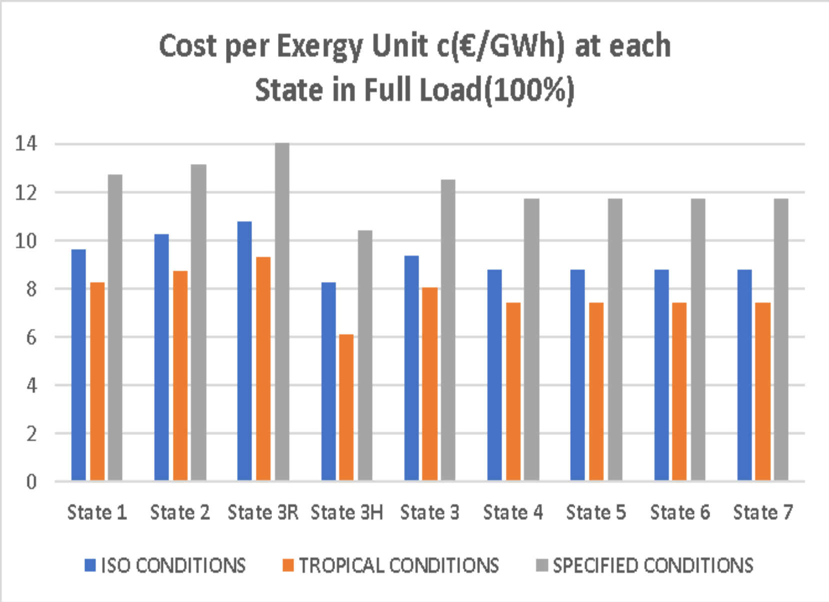

(a)

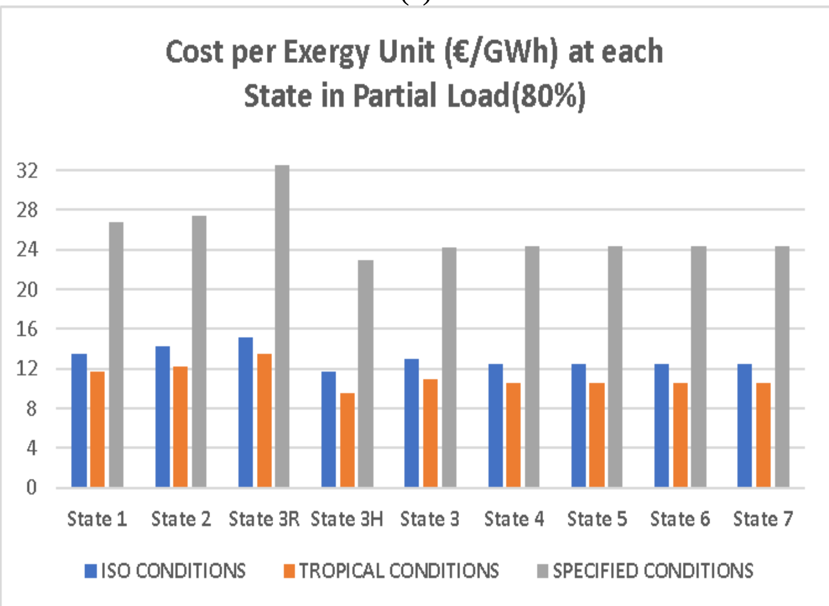

(b)

Figure 15. Variation of cost per exergy unit at each state (a) in full load , (b) in partial load in different environmental conditions

Figure 15 demonstrates the cost per exergy unit at each state of Split cycle in partial and in full load. As it is obvious, in Specified conditions every state has higher exergy unit cost in both loads. This can be explained because the physical exergy in these conditions is less than the other conditions. The lowest values are depicted in tropical conditions. As far as the states of the Split cycle, the highest exergy unit cost is illustrated at state 3R and the lowest exergy unit cost at state 3H in both loads.

11. Conclusions

In the present study 3 different CO_2 Supercritical Cycles were simulated in the engineering software EES. For these Supercritical Cycles a thermoeconomic analysis was carried out. Subsequently, the genetic algorithm was applied to them so as to optimize their functional parameters and find out the Cycle with the lowest EPC. For the Cycle with the lowest EPC a parametric analysis was carried out in order to demonstrate the variation of its efficiency in different engine loads. Finally, an Exergoeconomic and an Exergoenvironmental Analysis were performed in order to calculate the cost of the exergetic flows and various exergoenvironmental indicators . The optimization method utilizing the genetic algorithm demonstrated that the Supercritical Cycles have low production electricity cost despite the high installation cost.The main reason is that these Cycles are high energy efficient and lead to high production of power,in our study the production reaches 2MW. The application of the Genetic Algorithm in the optimization method also depicted that between these Supercritical Cycles, the Split Supercritical CO_2 cycle shows the lowest EPC. The optimization process showed that the minimization of the cost of the produced electricity is not proportionate to the maximization of the net produced power of the system but it requires to keep balance between the net produced power and the cost of the installation. The parametric analysis demonstrated that as the engine load increases, the bsfc is improved more, it is generated more power and the efficiency of the system increases.Finally, the Exergoeconomic Analysis depicted that the most costly exergy streams are in the states of the Cycle ,where the stream has the maximum exergy. To conclude, the waste heat recovery systems show great potential in the attempt to decrease the carbon dioxide emissions of a ship and to accomplish the strict IMO regulations. It should not be ignored the fact that these systems also lead to an important decrease of the travel cost of a ship, which is its major operating cost. The main drawback in these systems is their high installation cost. As far as the Supercritical CO_2 Cycles are concerned, the high amounts of generated power lead to low cost of the produced electricity and make this investement feasible.

References

1. CEAS Engine Calculations - MAN B&W - MAN Energy Solutions, Available online: https://marine.man-es.com/two-stroke/ceas (accessed 10 December 2021).
2. Choi, B.C., Kim, Y.M., 2013. Thermodynamic analysis of a dual loop heat recovery system with trilateral cycle applied to exhaust gases of internal combustion engine for propulsion of the 6800 TEU container ship. Energy 58, 404–416. https://doi.org/10.1016/j.energy.2013.05.017
3. Liu, L., Yang, Q., Cui, G., 2020. Supercritical Carbon Dioxide(s-CO2) Power Cycle for Waste Heat Recovery: A Review from Thermodynamic Perspective. Processes 8, 1461. https://doi.org/10.3390/pr8111461
4. Zahedi, E., Woerz, C., Reichardt, G., Umlauf, G., Liewald, M., Barz, J., Weber, R., Graf, T., 2018. Lubricant-free deep drawing using CO2 and N2 as volatile media injected through laser-drilled microholes. MATEC Web Conf. 190, 14007. https://doi.org/10.1051/matecconf/201819014007
5. Wang, X., Dai, Y., 2016. Exergoeconomic analysis of utilizing the transcritical CO2 cycle and the ORC for a recompression supercritical CO2 cycle waste heat recovery: A comparative study. Applied Energy 170, 193–207. https://doi.org/10.1016/j.apenergy.2016.02.112
6. Yang, X.-S., 2020. Nature-inspired optimization algorithms, 1st ed. Elsevier Inc, San Diego.
7. Cao, E., 2010. Heat transfer in process engineering. McGraw-Hill, New York.
8. Yang, F., Cho, H., Zhang, H., Zhang, J., 2017. Thermoeconomic multi-objective optimization of a dual loop organic Rankine cycle (ORC) for CNG engine waste heat recovery. Applied Energy 205, 1100–1118. https://doi.org/10.1016/j.apenergy.2017.08.127
9. García-Cascales, J.R., Vera-García, F., Corberán-Salvador, J.M., Gonzálvez-Maciá, J., 2007. Assessment of boiling and condensation heat transfer correlations in the modelling of plate heat exchangers. International Journal of Refrigeration 30, 1029–1041. https://doi.org/10.1016/j.ijrefrig.2007.01.004
10. Turton, R. (Ed.), 2018. Analysis, synthesis, and design of chemical processes, 5th edition. ed, Prentice Hall international series in the physical and chemical engineering sciences. Prentice Hall, Boston.
11. Lee, S.H., Lim, D.-H., Park, K., 2020. Optimization and Economic Analysis for Small-Scale Movable LNG Liquefaction Process with Leakage Considerations. Applied Sciences 10, 5391. https://doi.org/10.3390/app10155391
12. Yang, M.-H., Yeh, R.-H., 2015. Thermodynamic and economic performances optimization of an organic Rankine cycle system utilizing exhaust gas of a large marine diesel engine. Applied Energy 149, 1–12. https://doi.org/10.1016/j.apenergy.2015.03.083
13. Yan, Y.-Y., Lin, T.-F., 1999. Evaporation Heat Transfer and Pressure Drop of Refrigerant R-134a in a Plate Heat Exchanger. Journal of Heat Transfer 121, 118–127. https://doi.org/10.1115/1.2825924
14. Nafey, A.S., Sharaf, M.A., 2010. Combined solar organic Rankine cycle with reverse osmosis desalination process: Energy, exergy, and cost evaluations. Renewable Energy 35, 2571–2580. https://doi.org/10.1016/j.renene.2010.03.034

15. Thanganadar, D., Asfand, F., Patchigolla, K., 2019. Thermal performance and economic analysis of supercritical Carbon Dioxide cycles in combined cycle power plant. Applied Energy 255, 113836. https://doi.org/10.1016/j.apenergy.2019.113836
16. Ghaebi, H., Parikhani, T., Rostamzadeh, H., Farhang, B., 2017. Thermodynamic and thermoeconomic analysis and optimization of a novel combined cooling and power (CCP) cycle by integrating of ejector refrigeration and Kalina cycles. Energy 139, 262–276. https://doi.org/10.1016/j.energy.2017.07.154
17. Yang, X.-S., 2020. Nature-inspired optimization algorithms, 1st ed. Elsevier Inc, San Diego.
18. Mohammed, R.H., Ibrahim, M.M., Abu-Heiba, A., 2021. Exergoeconomic and multi-objective optimization analyses of an organic Rankine cycle integrated with multi-effect desalination for electricity, cooling, heating power, and freshwater production. Energy Conversion and Management 231, 113826. https://doi.org/10.1016/j.enconman.2021.113826
19. Yilmaz, C., Kanoglu, M., Abusoglu, A., 2015. Exergetic cost evaluation of hydrogen production powered by combined flash-binary geothermal power plant. International Journal of Hydrogen Energy 40, 14021–14030. https://doi.org/10.1016/j.ijhydene.2015.07.031
20. Zare, V., Mahmoudi, S.M.S., Yari, M., 2015. On the exergoeconomic assessment of employing Kalina cycle for GT-MHR waste heat utilization. Energy Conversion and Management 90, 364–374. https://doi.org/10.1016/j.enconman.2014.11.039
21. Wang, X., Dai, Y., 2016. Exergoeconomic analysis of utilizing the transcritical CO2 cycle and the ORC for a recompression supercritical CO2 cycle waste heat recovery: A comparative study. Applied Energy 170, 193–207. https://doi.org/10.1016/j.apenergy.2016.02.112
22. . Bejan, A., Tsatsaronis, G., Moran, M.J., 1996. Thermal design and optimization. Wiley, New York.
23. Ratlamwala, T.A.H., Dincer, I., Reddy, B.V., 2013. Exergetic and Environmental Impact Assessment of an Integrated System for Utilization of Excess Power from Thermal Power Plant, in: Dincer, I., Colpan, C.O., Kadioglu, F. (Eds.), Causes, Impacts and Solutions to Global Warming. Springer New York, New York, NY, pp. 803–824. https://doi.org/10.1007/978-1-4614-7588-0_42
24. Midilli, A., Dincer, I., 2009. Development of some exergetic parameters for PEM fuel cells for measuring environmental impact and sustainability. International Journal of Hydrogen Energy 34, 3858–3872. https://doi.org/10.1016/j.ijhydene.2009.02.066
25. Abbaspour, H., Ehyaei, M.A., Ahmadi, A., Panahi, M., Abdalisousan, A., Mirzohosseini, A., 2021. Energy, exergy, economic, exergoenvironmental and environmental (5E) analyses of the cogeneration plant to produce electrical power and urea. Energy Conversion and Management 235, 113951. https://doi.org/10.1016/j.enconman.2021.113951
26. Liu, P., Shu, G., Tian, H., 2019. How to approach optimal practical Organic Rankine cycle (OP-ORC) by configuration modification for diesel engine waste heat recovery. Energy 174, 543–552. https://doi.org/10.1016/j.energy.2019.03.016
27. LOGISTICS, D.O.T.AND.U.N.C.O.T.A.D., 2022. REVIEW OF MARITIME TRANSPORT 2021. UNITED NATIONS, S.l.
28. Smith, T.W.P.; Jalkanen, J.P.; Anderson, B.A.; Corbett, J.J.; Faber, J.; Hanayama, S.; O'Keeffe, E.; Parker, S.; Johansson, L.; Aldous, L.; et al. Third IMO Greenhouse Gas Study 2014; The International Maritime Organisation: London, UK, 2015.
29. Joung, T.-H., Kang, S.-G., Lee, J.-K., Ahn, J., 2020. The IMO initial strategy for reducing Greenhouse Gas(GHG) emissions, and its follow-up actions towards 2050. Journal of International Maritime Safety, Environmental Affairs, and Shipping 4, 1–7. https://doi.org/10.1080/25725084.2019.1707938
30. Jouhara, H., Khordehgah, N., Almahmoud, S., Delpech, B., Chauhan, A., Tassou, S.A., 2018. Waste heat recovery technologies and applications. Thermal Science and Engineering Progress 6, 268–289. https://doi.org/10.1016/j.tsep.2018.04.017

31. Liu, P., Shu, G., Tian, H., 2019. Carbon Dioxide as Working Fluids in Transcritical Rankine Cycle for Diesel Engine Multiple Waste Heat Recovery in Comparison to Hydrocarbons. J. Therm. Sci. 28, 494–504. https://doi.org/10.1007/s11630-019-1090-z
32. Nami, H., Mahmoudi, S.M.S., Nemati, A., 2017. Exergy, economic and environmental impact assessment and optimization of a novel cogeneration system including a gas turbine, a supercritical CO 2 and an organic Rankine cycle (GT-HRSG/SCO 2). Applied Thermal Engineering 110, 1315–1330. https://doi.org/10.1016/j.applthermaleng.2016.08.197
33. Liu, L., Yang, Q., Cui, G., 2020. Supercritical Carbon Dioxide(s-CO2) Power Cycle for Waste Heat Recovery: A Review from Thermodynamic Perspective. Processes 8, 1461. https://doi.org/10.3390/pr8111461
34. Wang, X., Yang, Y., Zheng, Y., Dai, Y., 2017. Exergy and exergoeconomic analyses of a supercritical CO2 cycle for a cogeneration application. Energy 119, 971–982. https://doi.org/10.1016/j.energy.2016.11.044
35. Pan, P., Yuan, C., Sun, Y., Yan, X., Lu, M., Bucknall, R., 2020. Thermo-economic analysis and multi-objective optimization of S-CO2 Brayton cycle waste heat recovery system for an ocean-going 9000 TEU container ship. Energy Conversion and Management 221, 113077. https://doi.org/10.1016/j.enconman.2020.113077
36. Su, R., Yu, Z., Xia, L., Sun, J., 2020. Performance analysis and multi-objective optimization of an integrated gas turbine/supercritical CO2 recompression/transcritial CO2 cogeneration system using liquefied natural gas cold energy. Energy Conversion and Management 220, 113136. https://doi.org/10.1016/j.enconman.2020.113136
37. Xia, W., Huo, Y., Song, Y., Han, J., Dai, Y., 2019. Off-design analysis of a CO2 Rankine cycle for the recovery of LNG cold energy with ambient air as heat source. Energy Conversion and Management 183, 116–125. https://doi.org/10.1016/j.enconman.2018.12.098
38. Kim, Y.M., Sohn, J.L., Yoon, E.S., 2017. Supercritical CO 2 Rankine cycles for waste heat recovery from gas turbine. Energy 118, 893–905. https://doi.org/10.1016/j.energy.2016.10.106